Arabian Journal for Science and Engineering (2024) 49:11479–11499
https://doi.org/10.1007/s13369-023-08703-x

RESEARCH ARTICLE-MECHANICAL ENGINEERING

Piezoelectric Actuator/Patch-Based Hybrid Repair and Fatigue Life Expansion of a Double-Edged Damaged Plate: An Analytical Approach and Numerical Validation

Sourav Pattanayak[1,2] · **Goutam Roy**[3] · **G. Pohit**[2]

Received: 6 September 2023 / Accepted: 28 December 2023 / Published online: 4 February 2024

Abstract
This study examines the use of piezoelectric materials/patches for passive, active, and hybrid repairs of a double-edged cracked plate. The study considers the stiffness effect of the piezoelectric patch for passive repair, the actuation effect of piezoelectric materials for active repair, and their combination as hybrid repair. The analytical model for cracked structures is developed using linear elastic fracture mechanics, which calculates the stress intensity factor (SIF) for various repair techniques under constant tensile load. The passive effect of the piezoelectric patch is determined using Rose's equations, while the stress produced by the piezoelectric material is computed using the weight function method. The fatigue life cycle for various repair configurations is determined under cyclic tensile loading using the Paris law with a stress ratio (R) of 0.1 and different voltage ratios (VR). The model is verified with experimental results and analytical fatigue life with FE solutions using ABAQUS software. It is to be noted that an analytical model is developed for the first time to account for both passive and active repairs, i.e., hybrid repair, and to verify the efficacy of the model using published experimental and FE solutions using ABAQUS. A parametric study is conducted to choose the best-sized piezoelectric actuator/patch, voltage, and voltage ratio. The results show a significant reduction in Mode-I SIF for all repair cases, with hybrid repair achieving the greatest reduction and extending fatigue life by 174.88, 116.23, and 37.92% as compared to without repair, active, and passive repairs, respectively, under 500 V with zero VR application.

Keywords Stress intensity factor (SIF) · Linear elastic fracture mechanics (LEFM) · Fatigue crack growth rate (FCGR) · Cracked plate · Piezoelectric actuator · Active repair · Stress ratio (R)

List of symbols

K_I	SIF of the cracked plate without repair
σ_0	Uniaxial tensile load
a	Crack length
W	Half-width of the plate
$F\left(\frac{a}{W}\right)$	Non-dimensional geometry correction factor
σ_P	Reduced stress at the crack plane after fixing the patch
σ_R	Stress developed in the patch
A	Cross-sectional area of the plate
A_R	Cross-sectional area of the patch
S	Stiffness ratio
E_P	Young's modulus of the patch
t_P	Thickness of the patch
W_P	Half-width of the patch
E	Young's modulus of the plate
t	Thickness of the plate
c	Physical parameter related to passive repair
k	Spring constant
υ	Poisson's ratio of the plate
β	Shear stress transfer length
G_A	Shear modulus of the adhesive material
t_A	Adhesive thickness
y_{max}	The distance of the extreme fibers of the cracked plate from the neutral axis
I_{Plate}	Moment of inertia of the plate

✉ G. Pohit
gpohit@gmail.com

[1] Department of Mechanical Engineering, Haldia Institute of Technology, Haldia 721657, India

[2] Department of Mechanical Engineering, Jadavpur University, Kolkata 700032, India

[3] Department of Mechanical Engineering, Narula Institute of Technology, Kolkata 700109, India

I_{Patch}	Moment of inertia of the patch
n	Ratio of modulus of elasticity
K_{P}	SIF after passive repair
K_{P}^{*}	Modified SIF of passive repair after considering bending effect
K_{A}	SIF after active repair
K_{Piezo}	SIF due to the actuation of the piezoelectric patch
$h(x, y, a)$	Weight function
$\sigma_{\text{Piezo}}(x)$	Stress produced by the piezoelectric patch
K_{H}	SIF after hybrid repair
$\frac{\text{d}a}{\text{d}N}$	Fatigue crack growth rate
C, m	Paris constants
$\sigma_{\max}$	Maximum applied stress
$\sigma_{\min}$	Minimum applied stress
$\Delta\sigma$	Stress range ($\sigma_{\max} - \sigma_{\min}$)
$K_{\max}$	Maximum SIF corresponds to maximum stress
$K_{\min}$	Minimum SIF corresponds to minimum stress
ΔK	SIF range ($K_{\max} - K_{\min}$)
a_{c}	Critical crack length
a_{o}	Initial crack length
K_{IC}	Fracture toughness
T	Width of the distributed electrode
d_{31}	Piezoelectric strain coefficient
ψ	Non-dimensional parameter related to stress developed by piezoelectric patch
α	A constant related to piezoelectric stress
$V_{\max}$	Maximum applied voltage
$V_{\min}$	Minimum applied voltage
ΔV	Difference in voltage ($V_{\max} - V_{\min}$)
$(\sigma_{\text{Piezo}})_{\max}$	Maximum stress produced by the piezoelectric patch under $V_{\max}$
$(\sigma_{\text{Piezo}})_{\min}$	Minimum stress produced by the piezoelectric patch under $V_{\min}$
$\Delta\sigma_{\text{Piezo}}$	Range of stress produced by the piezoelectric patch $\left[(\sigma_{\text{Piezo}})_{\max} - (\sigma_{\text{Piezo}})_{\min}\right]$
SIF	Stress intensity factor
GCF	Geometry correction factor
BCF	Bending correction factor
FCGR	Fatigue crack growth rate
WFM	Weight function method

1 Introduction

Any type of damage to a structural component results in its inability to function. In most cases, failure is caused by a damaged structure due to ongoing fatigue stress. In addition, a damaged structure experiences higher vibration, a substantial drop in overall loading capacity, and possibly total breakdown. Damage restoration is an economic way of extending the useful life of damaged components. Composite and metallic patch technique effectively heals structural fractures [1, 2]. A novel approach involves attaching piezoelectric actuators to damaged structures and controlling actuation using an external voltage [3]. Ouinas et al. [4] used the FE technique to show that two composite patches reduce the crack tip stress intensity factor (SIF), while the perpendicular orientation of fibers affects crack growth. A computational model had been developed [5] for optimizing composite patch repair in aluminum plates with core cracks, considering stacking sequences and material parameters. Various cost-effective and energy-efficient repair techniques [6–9] with FRP and composite patch show that the SIF is influenced by stress, crack geometry, material properties of the structure, patch, and adhesive materials.

Crawley et al. [10] discussed advancements in piezoelectric actuators for intelligent structures and static and dynamic models have been developed to predict structural reactions to command voltage. Wang et al. [11] proposed a method for repairing cracked beams using piezoelectric material's electro-mechanical characteristic, resulting in a local moment. Buckling capacity can be enhanced in cracked column structures [12]. A dynamically loaded cracked beam that had been repaired with piezoelectric material shows a decrease in stress singularity and a dynamic response [13]. An experimental study [13] found that piezoelectric patches effectively repair notched cantilever beams by monitoring crack severity using a sensor and applying voltage to actuator patches accordingly. Liu [14] investigated 2-D plane strain FE calculations for active crack repair using multilayered piezoelectric patches. Another repair study [15] was conducted using slope continuity and fracture mechanics criteria, and it was revealed that the fracture mechanics criteria are preferred for determining proper repair voltage. The repair of delaminated plates using piezoelectric patches was investigated by reducing tensile and compressive stresses and proposed the design of discrete electrodes, as well as assessing proper repair voltage [16]. Besides, it was proposed to use piezoelectric patches as a closed-loop feedback control repair method for vibrating delaminated beam systems [17]. Alaimo et al. [18] investigated the connection between the elastic and electric fields using the boundary element code of an active repaired structure and the impact of inertial forces. Wang et al. [19] recommended analytical methods to compute the interface stresses and energy release rates of a straight crack in a piezoelectric composite adhesive interface. The ideal placement for piezoelectric actuators and the effects of stiffness and thickness ratios to lower the SIF were examined by Fesharaki et al. [20, 21]. The effect of piezoelectric actuators on Mode-I active repair in thin plate structures was investigated by Abuzaid et al. [22], and SIF was calculated using LEFM. A piezoelectric patch effectively

reduces the SIF when used in extension mode. An experimental study had been implemented to confirm the model's accuracy [23]. The weight function method (WFM) was used to develop an analytical model of the SIF of a center-cracked plate caused by piezoelectric actuator stress, and FE simulation was performed to verify the model [24]. Roy et al. [25–27] developed an analytical model and finite element analysis to monitor damage in short and slender beams and presented non-destructive methods to identify cracks in structural components using a piezoelectric sensor. A model for restoring dynamic response utilizing steady-state vibration analysis and piezoelectric material was also proposed.

Composites and various FRP patches are used in a variety of repair studies. Service life can be enhanced by bonding single-sided composites on cracked structures [28]. Thickness, length, and the placement of the patch are the elements that influence fatigue life increase [29]. An experimental study [30] based on two-sided repair panels leads to reduced crack formation and improved fatigue life with high modulus CFRP sheets. Another experimental study [31] investigated FRP reinforcement on surface-cracked steel plates underneath repeated tension, revealing improved reinforcement quality and an optimal bond layer number. Double-sided repairs extend service life by over two times [32]. A study estimates a double symmetric patch's beneficial effect on fixing inclined cracks using the FE method, highlighting adhesive, patch, and plate properties [33]. An alternative solution [34] demonstrated the improved repair performance with hybrid composite patches for cracked aluminum 6061-T6 by reducing J-Integral and interfacial stresses. Hafiz et al. [35] examined the lifetime of joints with adhesive bonds during Mode-I fracture using stress life and fatigue crack growth approaches. Naghipour [36] investigated mixed-mode fatigue delamination in multidirectional composite laminates, highlighting interfacial cracking. The fatigue life of steel pipes/tubes with the presence of various surface cracks can be prolonged after strengthening with composite system repair (CRS) [37–39].

Cracking of steel can be successfully delayed by combining the strengthening effects of shape memory alloys (SMAs) with carbon fiber-reinforced polymers (CFRPs) [39]. The fatigue behavior of 2024 T3 v-notched specimens under different stress levels was studied by Albedah et al. [40]. Providing stop holes along crack sides in conjunction with FRP reinforcement resulted in a lower rate of crack growth and a longer fatigue life [41, 42]. The fatigue life of cracked structures with non-pre-stressed and pre-stressed bonded/wrapped CFRP plates under cyclic loads improves [43, 44].

The repair of cracked components can be performed using the composite patch, actuation effect by piezoelectric materials, stop hole technique, and the combination of stop hole and FRP patches under different types of loading. Even though composite patch repair has been widely investigated and proved to be very effective, the severity of the crack cannot be adjusted as the loading scenario changes. Due to this reason, the use of piezoelectric materials has become so popular nowadays as repair can be controlled by the externally applied voltage as and when required. However, only a few investigations have revealed the combined effect of piezoelectric materials and other repair techniques.

To the best of the authors' knowledge, no analytical model that combines the passive and active effects (voltage effect) of piezoelectric materials has been developed. To attain additional benefits from piezoelectric materials, the stiffness effect of the patch can be combined with the active effect when the patch is placed on the cracked surface to reduce the severity of the crack. So, the focus of the present research work is to propose a model based on this novel approach for the first time and subsequently investigate the influence of passive and active repairs (hybrid repair) on cracked specimens under fatigue loading. It is observed that the Mode-I SIF is significantly reduced after repairing the damaged plate followed by this hybrid repair under static loading. The significance of passive effect plays an essential role in extending fatigue life. The positive aspects of this sort of hybrid repair are that a large range of potential repairs may be made by only fixing one patch on the cracked surface. The passive effect is sufficient to lower SIF and extend fatigue life for minor crack length under low loading scenarios. In a critical environment, this can be accomplished by supplying external voltage as required. The cracked plate is modeled using linear elastic fracture mechanics (LEFM). Rose's equation, together with the bending correction factor (BCF), is used to model the passive repair method. The weight function method (WFM) is considered for modeling active repair. Paris law [45] is used to determine the fatigue crack growth rate (FCGR) and the life of a structure.

The fundamental goal of this research work is to accomplish the following objectives:

- To develop an analytical model that accounts for both passive and active repairs, i.e., hybrid repair, and to verify the efficacy of the model using published experimental and FE solutions using ABAQUS.
- To perform a parametric study for determining the optimal feasible geometrical dimensions and the appropriate voltage ratio (VR) for effective repair.
- To predict the fatigue life in terms of loading cycles for cracked, passive repair, active repair, and hybrid repaired structures using Paris law.
- To evaluate the fatigue crack growth rate (FCGR) using the developed analytical model and to examine the performance of the hybrid repairs in connection with other repair methods.

2 Problem Description

In this investigation, a double-edged cracked infinite plate under cyclic tensile load has been utilized for evaluation as shown in Fig. 1. To mitigate the influence of the crack, a piezoelectric actuator/patch is placed on the crack surfaces/the high-stress region to utilize the passive and active effects as well. The actuator utilizes an external electric field to induce compression stress near the cracked front. Due to stress redistribution, it tends to mitigate crack singular stresses resulting reduction in SIF. Because of the linearity of the materials, the superposition concept is used. As long as loading remains uniform, the SIF for linear elastic materials is additive. Thus, the superposition approach permits SIF solutions for complicated configurations to be developed from basic examples with well-established solutions. The width of the crack is taken as the same as that of the cracked plate.

3 Analytical Approach

In this section, the methodology followed for the analytical model and subsequent analysis is described.

3.1 Formulation of SIF (K_I) Under Static Loading Without Repair

In order to determine SIF, Tada's theoretical approach [46] was employed. The expression of the Mode-I SIF is given by Eq. (1) based on linear elastic fracture mechanics (LEFM) of a cracked rectangular plate of infinite size where Mode-I is taken into account as the only operative opening mode.

$$K_I = \sigma_0 \sqrt{\pi a} \tag{1}$$

where σ_0 is the uniaxial tensile stress applied on the cross section of the plate at an infinite distance (Fig. 1) with crack length 'a.' When the geometry of the cracked body affects the crack length, considering the non-dimensional geometry correction factor (GCF), $F\left(\frac{a}{W}\right)$, the Mode-I SIF may be redefined as [46]

$$K_I = \sigma_0 \sqrt{\pi a}.F\left(\frac{a}{W}\right) \tag{2}$$

where 'W' is the half-width of the cracked plate and the expression for $F\left(\frac{a}{W}\right)$ is given by

$$F\left(\frac{a}{W}\right) = \frac{1.122 - 0.561\left(\frac{a}{W}\right) - 0.205\left(\frac{a}{W}\right)^2 + 0.47\left(\frac{a}{W}\right)^3 - 0.19\left(\frac{a}{W}\right)^4}{\sqrt{1-\frac{a}{W}}} \tag{3}$$

3.2 Formulation of SIF (K_P^*) Under Static Loading with Passive Repair

In the case of passive repair, a cracked structure is considered with a piezoelectric actuator/patch attached to the plate. However, no actuation voltage is applied. Based on the superposition concept, stress distribution between the plate and piezoelectric patch as shown in Fig. 2 can be given by

$$\sigma_0 A = \sigma_P A + \sigma_R A_R \tag{4}$$

where σ_P is the reduced effective stress along the potential crack route [6, 47] after fixing the piezoelectric patch under uniform uniaxial stress σ_0. σ_R is the stress developed in the patch, and A and A_R are the cross-sectional area of the plate and patch, respectively.

The reduced SIF is given by Eq. (5)

$$K_P = \sigma_P \sqrt{\pi a} \tag{5}$$

The 1-D theory of bonded joints [48] is utilized to get the reduced stress shared by the plate and is expressed by Eq. (6)

$$\sigma_P = \frac{\sigma_0}{1+S} \tag{6}$$

where S is the stiffness ratio between the patch and the cracked plate and is given by

$$S = \frac{E_P \cdot W_P \cdot t_P}{E \cdot W \cdot t} \tag{7}$$

where E, W, and t and E_P, W_P, and t_P are Young's modulus, half-width, and thickness of the cracked plate and the piezoelectric patch, respectively.

For an arbitrary crack length, the following equation has been developed to compute the SIF for an infinite cracked plate using a single-sided patch [48, 49].

$$K_P = \sigma_P \cdot \sqrt{\frac{\pi ac}{a+c}} \tag{8}$$

The detailed explanation of the above equation is described in Appendix A.

The equation has been modified considering the geometry of the cracked plate [46].

$$K_P = \sigma_P \cdot \sqrt{\frac{\pi ac}{a+c}} \cdot F\left(\frac{a}{W}\right) \tag{9}$$

The previously mentioned mathematical approaches for the study of cracked, adhesively bonded structures are for extensional loading, and it is assumed that both the cracked and patch layers have no bending stiffness. The existence

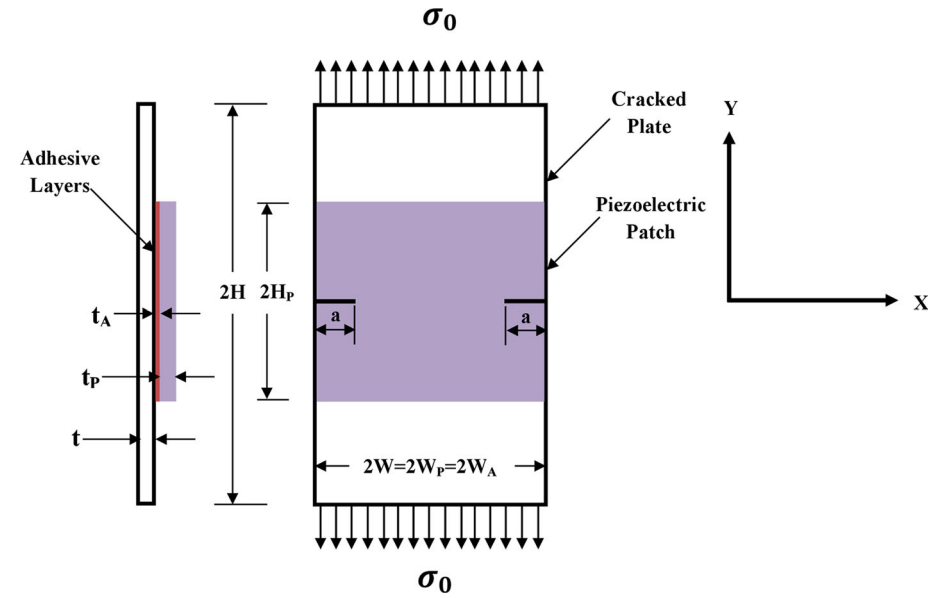

Fig. 1 Cracked plate repaired with piezoelectric actuator/patch

Fig. 2 Stress distribution between the plate and piezoelectric patch

of a crack in one layer of a bonded structure causes out-of-plane bending due to the loss of symmetry resulting from the crack. Out-of-plane bending enhances the stress intensity components. Bending's influence (increase in stress intensity parameters) in a structure develops as the crack length rises. This increase in stress intensity parameters will impact the propagation of fracture rates and must be taken into consideration in the study. The stress singularities in front of the crack tips eliminate the force transmitted at the cracking plane due to the existence of a crack in a single cracked layer. When such a cracked layer is part of an adhesively bonded structure, the same force release at the crack plane is taken in part by the cracked layer in the form of stress singularities, as with a single cracked layer, and the balance of the force is transmitted to the right next patch layer via the adhesive. The force in each plate near the plane of the cracking will differ from that at the ends due to the force transferred to the patch layer. At the crack's plane, the net internal unequal force between the two layers is equal to the force transferred from the crack to the patch layer. The bending can be attributed to this inconsistent force. Considering this bending effect, a bending correction factor (BCF) is introduced [1], and a modified SIF can be expressed by Eq. (10). The further details of BCF can be found in Appendix B.

$$K_P^* = (1 + \mathrm{BCF}) \cdot K_P \tag{10}$$

3.3 Formulation of SIF Under Static Loading with Active Repair (K_A) and Hybrid Repair (K_H)

3.3.1 Active Repair

SIF is calculated using the concept of superposition principle of LEFM, where two cases are taken into account and combined. The cases are described as follows: The cracked plate is subjected to mechanical loading only, and the plate is only under actuation (no mechanical loading). The SIF after active repair can be written as

$$K_A = K_I + K_{\mathrm{Piezo}} \tag{11}$$

where SIF under actuation effect K_{Piezo} is evaluated by weight function method (WFM) as proposed Bueckner [50] and K_I is computed in Sect. 3.1. The weight function is evaluated using the y-direction displacement as obtained by the Westergaard stress function [51]. Now the solution of K_{Piezo} may thus be obtained from the following statement for a cracked body using weight function h(x, y, a) and piezoelectric stress $\sigma_{\mathrm{Piezo}}(x)$ [23].

$$K_{\mathrm{Piezo}} = \int_0^a \{h(x, y, a) \cdot \sigma_{\mathrm{Piezo}}(x)\} \mathrm{d}x \tag{12}$$

The derivation of weight function h(x, y, a) and piezoelectric stress $\sigma_{\mathrm{Piezo}}(x)$ can be found in Appendix C.

As the solution obtained by Eq. (12) is based on the application of LEFM, the effect of the geometry of any infinite plate is to be taken into account using the dimensionless geometry correction factor proposed by Tada et al. [46] and

Eq. (12) is modified as

$$K_{\text{Piezo}} = \left[\int_0^a \{h(x,\ y,\ a) \cdot \sigma_{\text{Piezo}}\} \cdot \mathrm{d}x\right] \cdot F\left(\frac{a}{W}\right) \tag{13}$$

Now, using Eq. (2) and Eq. (13), K_A can be expressed as

$$K_A = \left[\sigma_0\sqrt{\pi a} + \int_0^a h(x,\ y,\ a) \cdot \sigma_{\text{Piezo}} \cdot \mathrm{d}x\right] \cdot F\left(\frac{a}{W}\right) \tag{14}$$

3.4 Hybrid Repair

The expression of SIF as represented by Eq. (14) holds good for active repair only i.e., the passive reinforcement effect is not considered. Since this research is not only concerned with active repair but also focuses on the passive effect it possesses, a concept of an innovative repair method is established that encompasses the idea of merging both repair methods and is termed a 'hybrid' repair. The superposition principle is used yet again by considering the cases: The plate is attached with a non-activated patch under mechanical loading (no voltage), and the plate is only under actuation (no mechanical loading). The SIF after hybrid repair can be written as $K_H = K_P^* + K_{\text{Piezo}}$ where K_P^* is calculated in Sect. 3.2 while K_{Piezo} is in the previous discussion. The final expression of SIF can be expressed as

$$K_H = \left[(1 + \text{BCF}) \cdot \frac{\sigma_0}{1+S} \cdot \sqrt{\frac{\pi \text{ac}}{a+c}} + \int_0^a h\,(x,\ y,\ a) \cdot \sigma_{\text{Piezo}} \cdot \mathrm{d}x\right] \cdot F\left(\frac{a}{W}\right) \tag{15}$$

3.5 Computation of Fatigue Life (N_f) and FCGR (da/dN) for the Cases: Without Repair (K_I), Passive (K_P^*), Active (K_A), and Hybrid Repair (K_H)

In this section, fatigue crack growth rate (FCGR) and service life of a cracked structure are estimated under cyclic tension. For this purpose, the Paris crack growth model for Mode-I is adopted and is expressed as

$$\frac{\mathrm{d}a}{\mathrm{d}N} = C \cdot (\Delta K)^m \tag{16}$$

The above expression gives the FCGR (mm/cycle). C and m are the material constants for a particular value of stress ratio (R).

The difference in SIF for maximum and minimum loading is necessary for this study and may be calculated using the previous sections' derivations. The change in SIF ($\Delta K = K_{\max} - K_{\min}$) is influenced by the change in stress quantity only ($\Delta\sigma = \sigma_{\max} - \sigma_{\min}$) in all cases under consideration, such as without repair, passive repair, active repair, and hybrid repair. To find out the fatigue life as well as the fatigue crack growth rate for all the above scenarios, Eq. (16) is integrated from initial crack length a_o to final crack lengtha_f. During numerical integration, a small incremental crack extension Δa_i is recorded for an incremental number of cycles ΔN_i and can be written as $a_{i+1} = a_i + \Delta a_i$ and $N_{i+1} = N_i + \Delta N_i$, respectively. Under cyclic tensile load, there is an increase in crack length and it reaches the value of critical crack length a_c ($a_f \rightarrow a_c$) after any number of loading cycles. To find the fatigue life of a damaged structure, the above-mentioned numerical integration is to be carried out between a_o and a_c. The fracture toughness of the plate material is given by $K_{IC} = \sigma_0 \cdot F\left(\frac{a_c}{W}\right)$. The critical length depends on the applied stress and configuration of the cracked structure.

Case 1. Without repair

From Eq. (2), the SIF range can be written as

$$\Delta K_I = \Delta\sigma \cdot \sqrt{\pi a} \cdot F\left(\frac{a}{W}\right) \tag{17}$$

Putting this value in Eq. (16), we have

$$\frac{\mathrm{d}a}{\mathrm{d}N} = C \cdot \left[\Delta\sigma \cdot \sqrt{\pi a}.F\left(\frac{a}{W}\right)\right]^m \text{ and } \mathrm{d}N = \frac{\mathrm{d}a}{C \cdot \left[\Delta\sigma \cdot \sqrt{\pi a}.F\left(\frac{a}{W}\right)\right]^m} \tag{18}$$

In order to calculate the propagated crack length after the N loading cycle, numerical integration of Eq. (18) is performed.

$$N_f = \int_0^{N_f} \mathrm{d}N = \int_{a_o}^{a_{f=a_c}} \frac{\mathrm{d}a}{C \cdot \left[\Delta\sigma \cdot \sqrt{\pi a}.F\left(\frac{a}{W}\right)\right]^m} \tag{19}$$

Case 2. Passive Repair

From Eq. (10), SIF range can be written as

$$\Delta K_P^* = (1 + \text{BCF}) \cdot \frac{\Delta\sigma}{1+S} \cdot \sqrt{\frac{\pi \text{ac}}{a+c}} \cdot F\left(\frac{a}{W}\right) \tag{20}$$

Putting this value in Eq. (16), we have

$$\frac{\mathrm{d}a}{\mathrm{d}N} = C \cdot \left[(1 + \text{BCF}) \cdot \frac{\Delta\sigma}{1+S} \cdot \sqrt{\frac{\pi \text{ac}}{a+c}} \cdot F\left(\frac{a}{W}\right)\right]^m \text{ and } \mathrm{d}N = \frac{da}{C \cdot \left[(1 + \text{BCF}) \cdot \frac{\Delta\sigma}{1+S} \cdot \sqrt{\frac{\pi \text{ac}}{a+c}} \cdot F\left(\frac{a}{W}\right)\right]^m} \tag{21}$$

In the same way, we can calculate the fatigue life after passive repair as

$$N_f = \int_0^{N_f} \mathrm{d}N = \int_{a_o}^{a_{f=a_c}} \frac{\mathrm{d}a}{C \cdot \left[(1+\mathrm{BCF}) \cdot \frac{\Delta\sigma}{1+S} \cdot \sqrt{\frac{\pi \mathrm{ac}}{a+c}} \cdot F\left(\frac{a}{W}\right)\right]^m} \tag{22}$$

Case 3. Active Repair

From Eq. (14), SIF range for only active repair can be written as

$$\Delta K_A = \left\{\Delta\sigma\sqrt{\pi a} + \int_0^a h\,(x,\, y,\, a) \cdot \Delta\sigma_{\mathrm{Piezo}} \cdot \mathrm{d}x\right\} \cdot F\left(\frac{a}{W}\right). \tag{23}$$

where

$$\Delta\sigma_{\mathrm{Piezo}} = \frac{EtT}{A\,(\psi+\alpha)} \frac{d_{31}}{t_P} \Delta V, \quad \text{and} \quad \Delta V = V_{\max} - V_{\min}.$$

Putting this value in Eq. (16), we haveand

$$\frac{\mathrm{d}a}{\mathrm{d}N} = C \cdot \left[\left\{\Delta\sigma\sqrt{\pi a} + \int_0^a h\,(x,\, y,\, a) \cdot \Delta\sigma_{\mathrm{Piezo}} \cdot \mathrm{d}x\right\} \cdot F\left(\frac{a}{W}\right)\right]^m$$

$$\mathrm{d}N = \frac{\mathrm{d}a}{C \cdot \left[\left\{\Delta\sigma\sqrt{\pi a} + \int_0^a h(x,\, y,\, a) \cdot \Delta\sigma_{\mathrm{Piezo}} \cdot \mathrm{d}x\right\} \cdot F\left(\frac{a}{W}\right)\right]^m} \tag{24}$$

and the fatigue life is given by

$$N_f = \int_0^{N_f} \mathrm{d}N = \int_{a_o}^{a_{f=a_c}} \frac{\mathrm{d}a}{C \cdot \left[\left\{\Delta\sigma\sqrt{\pi a} + \int_0^a h\,(x,\, y,\, a) \cdot \Delta\sigma_{\mathrm{Piezo}} \cdot \mathrm{d}x\right\} \cdot F\left(\frac{a}{W}\right)\right]^m} \tag{25}$$

Case 4. Hybrid Repair

From Eq. (15), SIF range can be written as

$$\Delta K_H = \left\{(1+\mathrm{BCF}) \cdot \frac{\Delta\sigma}{1+S} \cdot \sqrt{\frac{\pi \mathrm{ac}}{a+c}} + \int_0^a h\,(x,\, y,\, a) \cdot \Delta\sigma_{\mathrm{Piezo}} \cdot \mathrm{d}x\right\} \cdot F\left(\frac{a}{W}\right) \tag{26}$$

Putting this value in Eq. (16), we haveand

$$\frac{\mathrm{d}a}{\mathrm{d}N} = C \cdot \left[\left\{(1+\mathrm{BCF}) \cdot \frac{\Delta\sigma}{1+S} \cdot \sqrt{\frac{\pi \mathrm{ac}}{a+c}} + \int_0^a h(x,\, y,\, a) \cdot \Delta\sigma_{\mathrm{Piezo}} \cdot \mathrm{d}x\right\} \cdot F\left(\frac{a}{W}\right)\right]^m$$

$$\mathrm{d}N = \frac{\mathrm{d}a}{C \cdot \left[\left\{(1+\mathrm{BCF}) \cdot \frac{\Delta\sigma}{1+S} \cdot \sqrt{\frac{\pi \mathrm{ac}}{a+c}} + \int_0^a h\,(x,\, y,\, a) \cdot \Delta\sigma_{\mathrm{Piezo}} \cdot \mathrm{d}x\right\} \cdot F\left(\frac{a}{W}\right)\right]^m} \tag{27}$$

And the fatigue life is given by

Table 1 Parameters about the geometry of the repaired configurations as shown in Fig. 1

Dimensions	Al 2024-T3 (mm)	PZT-5H (mm)	Resin epoxy (mm)
Height	H = 200	$H_P = 100$	$H_A = 100$
Width	W = 100	$W_P = 100$	$W_A = 100$
Thickness	t = 1.6	$t_P = 0.5$, 0.75 and 1	$t_A = 0.05$, 0.075 and 1

$$N_f = \int_0^{N_f} \mathrm{d}N = \int_{a_o}^{a_{f=a_c}} \frac{\mathrm{d}a}{C \cdot \left[\left\{(1+\mathrm{BCF}) \cdot \frac{\Delta\sigma}{1+S} \cdot \sqrt{\frac{\pi \mathrm{ac}}{a+c}} + \int_0^a h\,(x,\, y,\, a) \cdot \Delta\sigma_{\mathrm{Piezo}} \cdot \mathrm{d}x\right\} \cdot F\left(\frac{a}{W}\right)\right]^m} \tag{28}$$

4 Finite Element Analysis by ABAQUS CAE

In order to validate the results obtained from the numerical analysis, an FE model is developed by modeling a structure with a piezoelectric patch.

At first, three deformable bodies are created and 2 planar shells are created to model the Plate, piezoelectric patch, adhesive layer, and cracks with the dimensions, material properties, and damage parameters as given in Tables 1–5. The plate model is partitioned into two geometries to incorporate the crack on both sides of the plate. The piezoelectric patch model is defined with a local material orientation by creating a datum where axis 3 is kept along the depth of the patch model. It is to be noted that ABAQUS takes direction 3 as the polarization direction. The piezoelectric patch and cracked plates are attached by using tie interaction under the interaction module. The model is simulated under a static step where the cyclic load is applied by creating a tabular amplitude and selecting the created amplitude as the variation in the magnitude of load with time. The external voltage on the piezoelectric patch is applied by creating two electrical boundary conditions on the two opposite faces of the patch. The voltage of the face attached to the adhesive is kept zero, and the other face is given a finite value. Subsequently, for validation purposes, three more deformable bodies are created under the part module to model the cracked plate and two piezoelectric patches with the dimensions as considered in the published literature by Abuzaid et al. [23]. For the analysis, material properties as mentioned in Ref. [23] are assigned to the plate model and piezoelectric patch models. Thenceforth, as required a seam crack at the middle of one side of the plate is considered.

The propagation of a crack is considered to be in quasi-static condition, i.e., the crack grows very slowly such that at every instant the problem can be considered static and can be

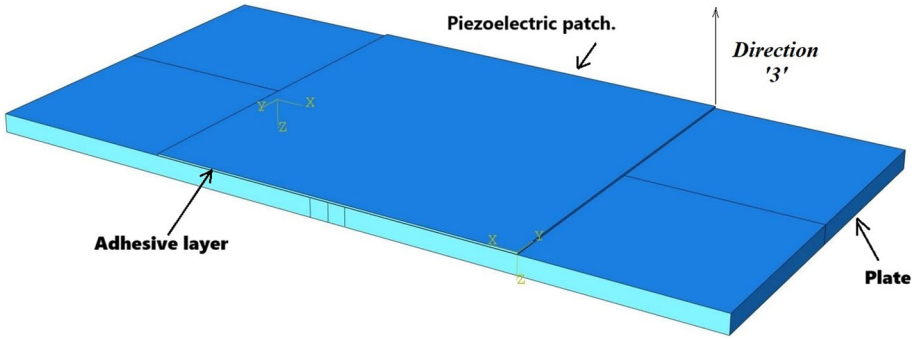

Fig. 3 Model of the cracked plate with an assembled piezoelectric patch on the ABAQUS platform

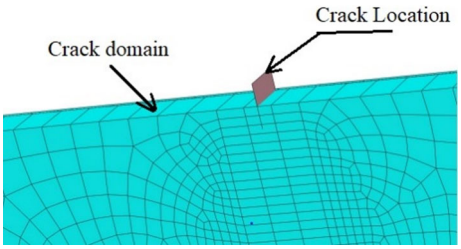

Fig. 4 Depiction of the crack domain, crack location, and meshing condition for XFEM analysis

performed by the extended finite element method (XFEM). Without re-meshing the model, XFEM enables the investigation of fracture growth along solution-dependent paths. The maximum principal stress value is specified to initiate the crack propagation in the material definition. XFEM analysis is performed under the static step. Figure 3 depicts the 3D model with the tied piezoelectric patch with an adhesive layer and the location of the crack. Figure 4 shows the selected crack domain and the planar element that is required to specify the XFEM crack.

5 Validation

5.1 Comparison of Analogous Experimental Result with Present Theoretical Analysis

In order to validate the efficacy of the present analytical approach and finite element analysis, results obtained by both methods are compared with the experimental and numerical results published in Ref. [23]. The material properties, geometric properties, loading conditions, and boundary conditions are considered identical to those of Ref. [23]. Two piezoelectric patches are bonded by an adhesive layer as shown in Fig. 5.

Figure 6a and b depicts the finite element model of the plate discretized by hexahedral elements and its deformed shape, respectively. Figure 7 presents the comparison of the present theoretical and FE analysis with the experimental results published by Abuzaid et al. [23]. It may be noted that the results of the present analysis match pretty well with that of the published literature.

5.2 Comparison of Present Analytical Result with the FE Analysis (ABAQUS)

The present analytical approach aims to intend that a piezoelectric patch can slow down the fatigue crack growth rate. In addition to the analytical approach, a finite element analysis (FEA) with the help of ABAQUS Standard CAE is performed to match the results. To facilitate the crack propagation under cyclic loading, XFEM (extended finite element) cracks are incorporated into the plate and the model is simulated under a static step. The model is discretized by hexahedral elements with 0.00015 m approximate global size. The sweep meshing technique with the medial axis algorithm is considered for discretization. In the static step, the cyclic load is applied by creating tabular amplitude which varies the load with time as required, where the maximum and minimum stress values are 330 and 33 MPa, respectively. The adhesive layer is sandwiched between the plate and the piezoelectric patch as mentioned in ref. [52, 53]. The mating faces of the adhesive layer to piezoelectric patch and adhesive layer to plates are assembled by using tie interaction from the interaction module. An electrical boundary condition of zero voltage is applied on the face of the piezoelectric patch which is attached with the adhesive layer.

For the analysis, the parameters related to the geometry of the plate, piezoelectric patch (PZT-5H), and adhesive are given in Table 1. The material properties are mentioned in Tables 2, 3 and 4, respectively. The fatigue properties of the plate Al 2024-T3 are given in Table 5.

It should be mentioned that 500 V is provided to the piezoelectric patch to slow down the crack propagation rate. Thereafter, the results are compared for authentication and the same are shown in Fig. 8. The graphical comparison between the results obtained by FEA and the analytical method shows a good match. The deformed FE models of the cracked plate with propagated crack before and after attaching the piezoelectric patch are shown in Fig. 9.

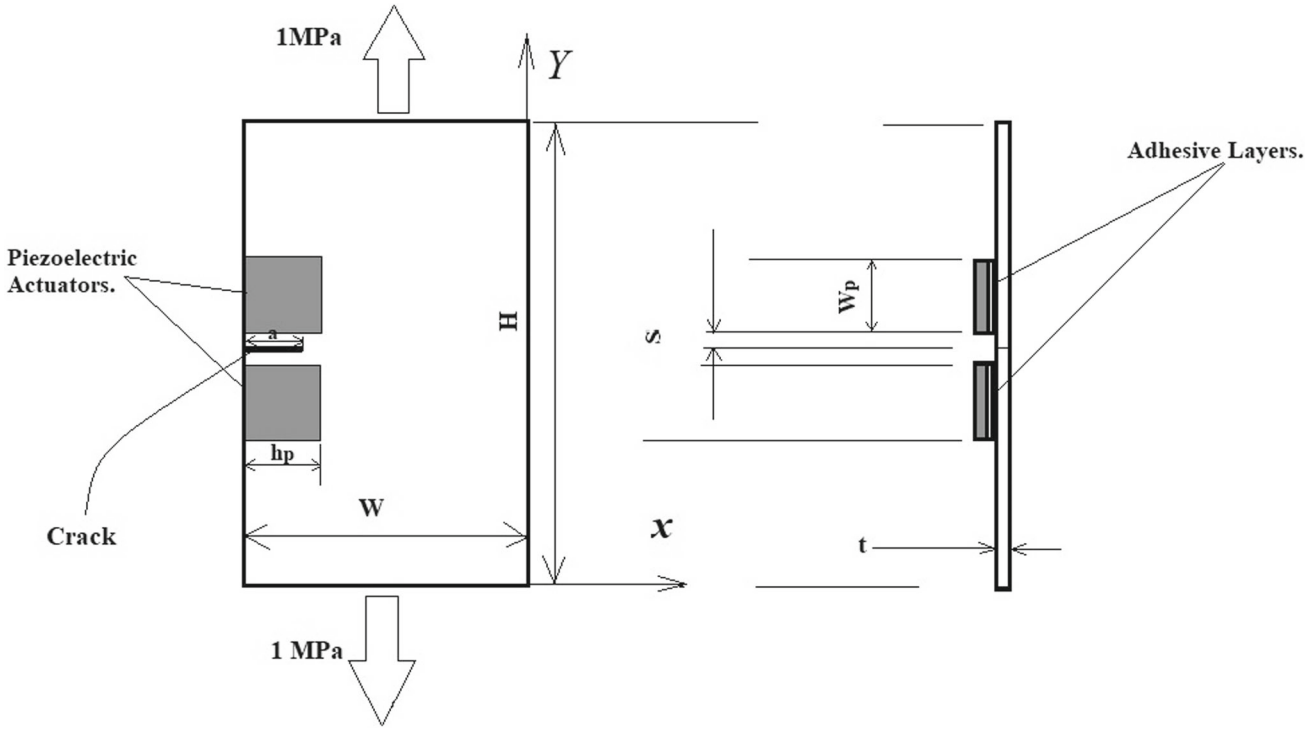

Fig. 5 Schematic illustration of the considered cracked plate with bonded piezoelectric patch as used in the experimental work of Abuzaid et al. [23]

The simulated finite element models at the three conditions without repair (without patch), passive repair (patch without voltage actuation), and active repair (with actuated patch) are depicted in Figs. 9a, b, and c.

6 Results and Discussions

Once the output of the numerical simulation is matched with the FE analysis, further investigation is carried out to determine the fatigue life and FCGR under cyclic loading without

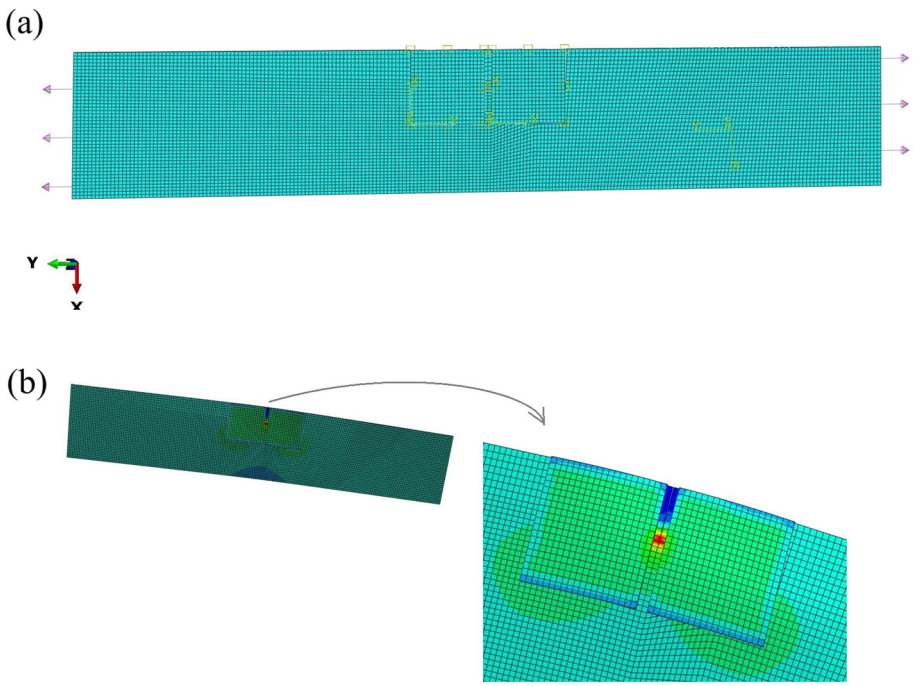

Fig. 6 FE model of the cracked plate with attached piezo actuators considered for validation **a** before simulation, **b** after simulation

Table 2 Mechanical properties of Al 2024-T3 plate material

Elastic modulus (E) (GPa)	Poisson's ratio (ν)	Tensile yield strength (MPa)	Ultimate tensile strength (MPa)	Density Kg/m^3
74	0.33	345	483	2780

Table 3 Properties of piezoelectric material PZT-5H

Piezoelectric coefficient (10^{-12} C/N)	Flexibility coefficient (10^{-12} m^2/N)	Dielectric constant	Density Kg/m^3
$d_{31} = -274$ $d_{33} = 593$ $d_{15} = 741$	$s_{11} = 16.5$, $s_{12} = -4.78$, $s_{14} = -8.45$, $s_{33} = 20.7$, $s_{44} = 43.5$, $s_{66} = 2(s_{11} - s_{12})$	$k_{11} = 3130$ $k_{31} = 3400$	7600

Table 4 Material properties of resin epoxy

Elastic modulus (E_A) (GPa)	Poisson's ratio ν_A	Tensile yield strength (T_A) (MPa)	Shera modulus (G_A) (GPa)	Density (Kg/m^3)
2.8	0.35	30	1.05	1210

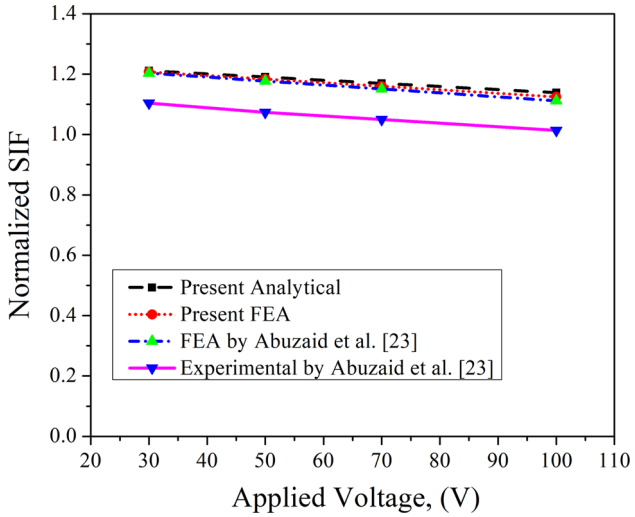

Fig. 7 Comparison of the present results with the published experimental and numerical results in Abuzaid et al. [23]

Table 5 Fracture properties of Al 2024-T3 and Paris law material constants at stress ratio R = 0.1

$\Delta K_{th}(MPa\sqrt{m})$	$K_{IC}(MPa\sqrt{m})$	C	m
3.61	33.16	7.172×10^{-8}	3.0089

repair, passive repair, active repair, and hybrid repair of the cracked plate using the analytical method proposed in this work.

6.1 Fatigue Life Without Repaired Plate

The cracked plate without repair (plate without patch) is subjected to a cyclic load between 8 KN and 0.8 KN, which results in $\sigma_{max} = 50$MPa, $\sigma_{min} = 5$MPa, and the stress ratio (SR) of 0.1. The same stress ratio is maintained for all the subsequent analyses. Crack length is propagated under fatigue loading and reaches the critical crack length of a_c, when $(K_I)_{Withoutrepair} = K_{IC}$. The corresponding number of cycles N_f provides the fatigue life which is calculated using Eq. (22). Figure 10a represents the increase in crack length without a repaired plate concerning the number of loading cycles (N), and Fig. 10b shows the change in FCGR (da/dN) against SIF range (ΔK).

6.2 Fatigue Life of Passive Repaired Plate

The bonded piezoelectric patch is attached to the plate. However, no voltage is applied to the patch. SIF is reduced significantly due to its passive effect i.e., due to stiffness of patch material. The fatigue life is calculated for passive repair using Eq. (24). This repair method is affected by the piezoelectric patch thickness, t_P, and adhesive thickness, t_A. To study the effect of thicknesses and to choose the best possible thicknesses of the patch and adhesive, an investigation is carried out for different patch thicknesses, $t_P = 0.5$, 0.75, and 1 mm, and different adhesive thicknesses $t_A = 0.05$, 0.075 and 0.1 mm

Figure 11 demonstrates the propagation of crack length with respect to the number of loading cycles for different patch and adhesive thicknesses. From Eq. (20), it is clear that da/dN provides a fixed value for a particular value of ΔK

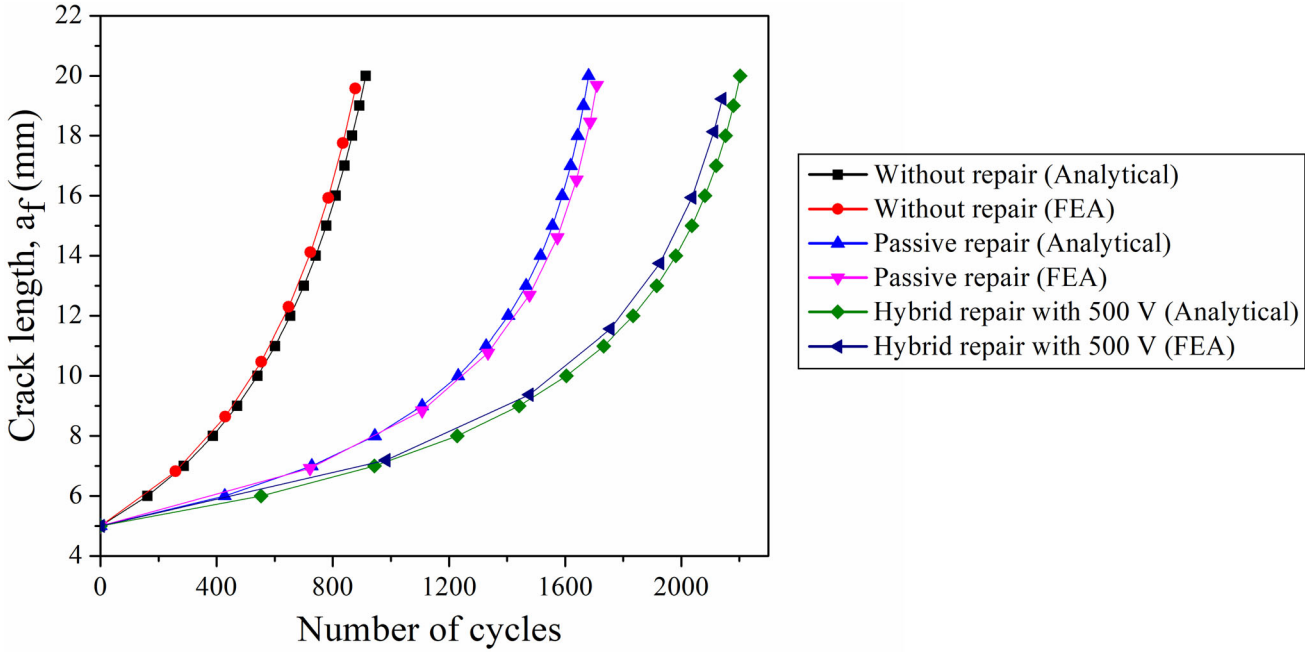

Fig. 8 Comparison of present analytical results with the results obtained by FEA in ABAQUS

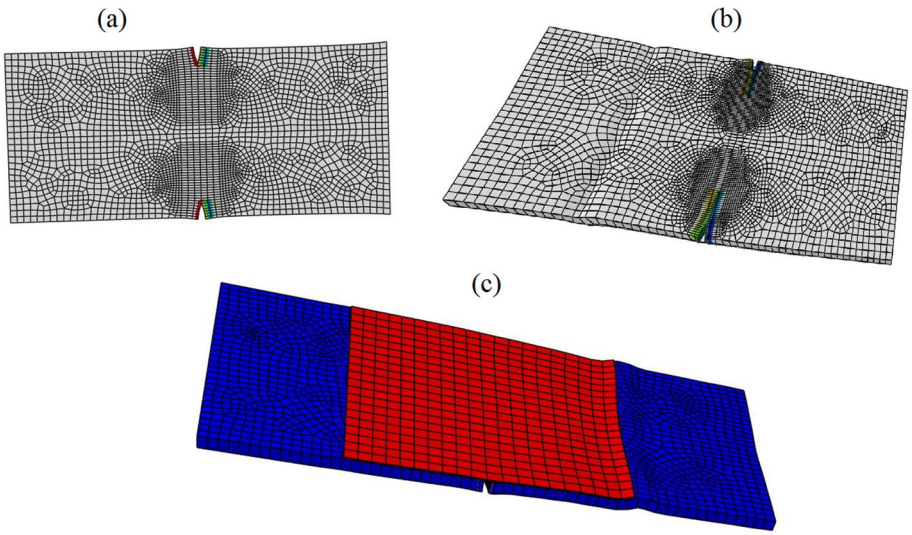

Fig. 9 Deformed FE model of the cracked plate with propagated crack **a** before attaching the piezoelectric patch, **b** after attaching the piezoelectric patch,**c** after attaching the piezoelectric patch and applying a voltage of 500 V

for all parameters related to different repair configurations. But ΔK attains a particular value after a different number of loading cycles for different configurations. Thus, for proper comparison of FCGR with respect to the SIF range, it is important to choose an optimum number of loading cycles. In this case, the change in FCGR (da/dN) with respect to SIF range (ΔK) within 3×10^5 cycles is shown in Fig. 12 for different adhesive thicknesses. The crack growth rate can be delayed by maintaining a higher patch thickness. The crack growth rate without repair plate is also included in the figure.

Figure 13 demonstrates the variation in fatigue life (N_f) for different patches and adhesive thicknesses. As can be seen, passive repair enhances the fatigue life by 99.31, 254, and 520% for patch thicknesses 0.5, 0.75, and 1 mm, respectively, as compared to without repair condition when the adhesive thickness is kept at 0.05 mm. For different adhesive thicknesses (0.075 and 0.1 mm), it is found that fatigue life can be enhanced by 68.56, 195.25, 411 and 51.73, 163.23, 351.95% as compared to without repair condition. The fatigue life is also increased by 77.6 and 211.5% for patch thickness 0.75 and 1 mm, respectively, as compared to the fatigue life obtained when patch thickness is 0.5 mm. This is found as better stress distribution occurs for higher patch thickness which results in lower crack tip stress and lower SIF and hence an increase in fatigue life. For passive repair of any

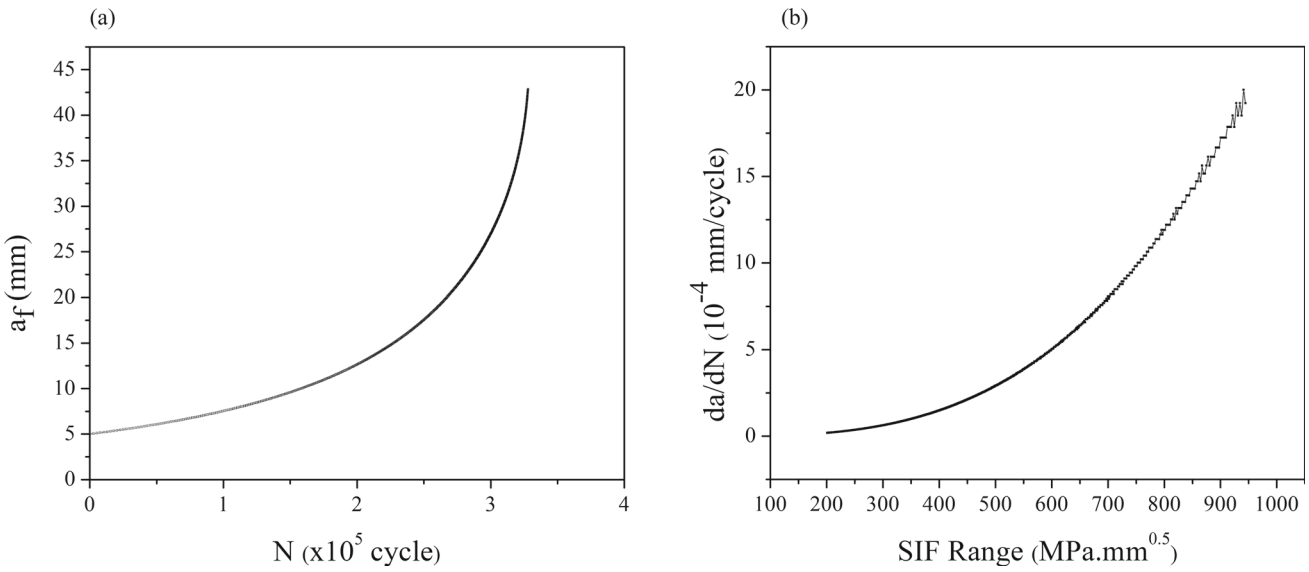

Fig. 10 Results of the without repaired plate **a** Final crack length vs. number of loading cycles, **b** fatigue crack growth rate vs. SIF range

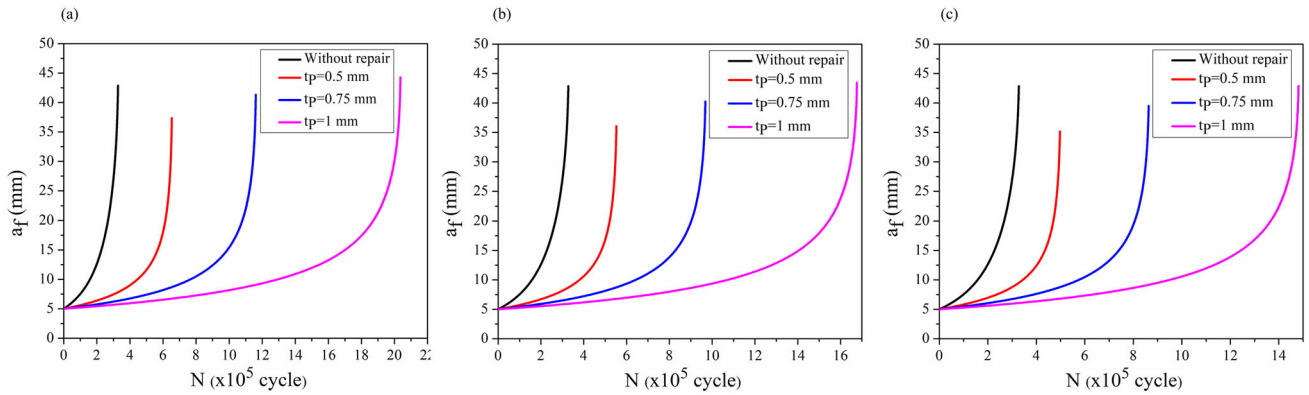

Fig. 11 Change in crack length with loading cycles for passive repair installation **a** $t_A = 0.05$ mm, **b** $t_A = 0.75$ mm **c** $t_A = 0.1$ mm

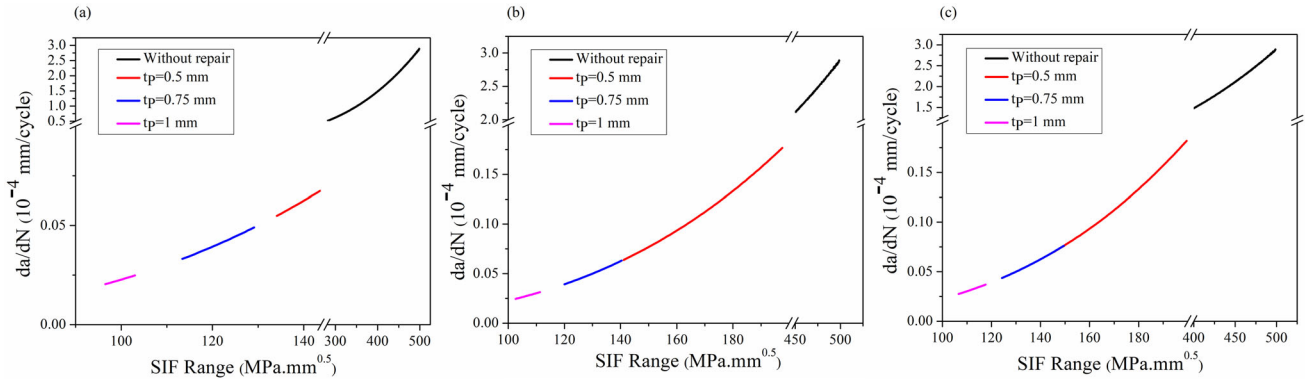

Fig. 12 Fatigue crack growth rate vs SIF Range for passive repair configuration **a**$t_A = 0.05$ mm, **b** $t_A = 0.75$ mm **c** $t_A = 0.1$ mm

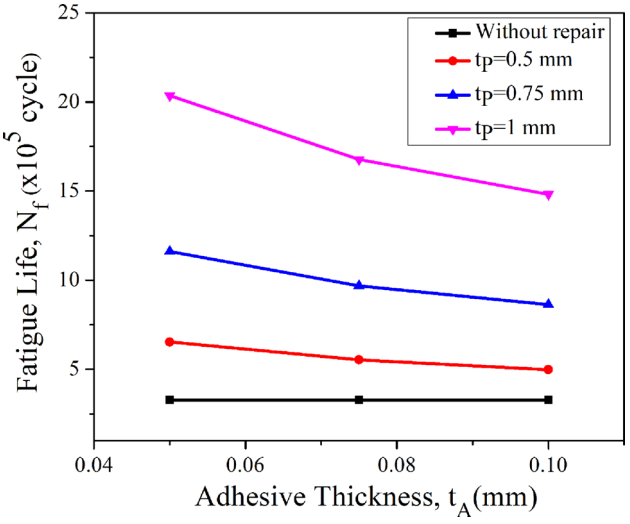

Fig. 13 Fatigue life vs. adhesive thickness for various patch thicknesses for a passive repair illustration

cracked structure, a higher thickness of the patch is found to be more efficient.

However, for a particular patch thickness, fatigue life decreases with the increase in adhesive thickness. Fatigue life is reduced by 15.4 and 23.8% for the adhesive thickness of 0.075 and 0.1 mm, respectively, as compared to the fatigue life obtained for the adhesive thickness of 0.05 mm when patch thickness is kept at 0.5 mm. This may be a consequence of inadequate load transfer to the patch, which results in the patch sharing reduced load. For low adhesive thickness, the crack growth rate is shown to be minimal as described in Fig. 12. So, for better repair performance thickness adhesive is to be chosen.

6.3 Fatigue Life of Active Repair

In this section, the repair performance of only actuation by the piezoelectric patch is discussed, neglecting the passive effect. This discussion is made to have the appropriate voltage ratio (VR), thickness, and externally applied voltage of the patch. For this analysis, the thickness of the adhesive is kept low say 0.05 mm as higher adhesive thickness leads to a decrease in the load transfer to the cracked plate and hence low repair performance.

6.3.1 Effect of Voltage Ratio (VR)

Since the repair method is carried out under fatigue loading, it is very important to choose the proper voltage ratio (VR = $V_{\min}/V_{\max}$) applied to the patch for better performance. The fatigue crack growth rate depends on the SIF range (ΔK), and the fatigue life additionally depends on K_{max} as fatigue life is calculated when K_{max} becomes equal to the K_{IC}. So, minimizing SIF range (ΔK) and maximizing the number of cycles required to reach the fracture toughness ($K_{\max} = K_{IC}$) are the significant attention of this analysis. Voltage ratio (VR) is taken as 0, 0.2, 0.4, 0.6, 0.8, and 1.0 with $V_{\max}$ = 500V.

The change in crack length against the loading cycle is shown in Fig. 14a for various voltage ratios. Because the maximum voltage is fixed in this case, the maximum SIFs are the same for all voltage ratios, and thus, the critical crack length is identical. It is observed that the number of loading cycles required to reach the critical crack length (a_c = 43.77 mm) drops with a rising voltage ratio. Figure 14b illustrates the change in the rate of fatigue development of cracks about the SIF range (ΔK) within 10^5 cycles, and it indicates that the voltage ratio has a significant influence on crack growth rate and that the zero voltage ratio (VR = 0 or $V_{\min}$ = 0) offers the most delayed crack growth.

It is observed that the maximum fatigue life is obtained when VR = 0 and it decreases as VR increases, while $V_{\max}$ is kept constant at 500 V. The fatigue life is improved by 27.12, 21, 15.28, 9.92, 4.85, and 0.12% corresponding to VR = 0, 0.2, 0.4, 0.6, 0.8, and 1, respectively, as compared to without repair cases as shown in Fig. 14c. For active repair,

$$\Delta K = \left\{ \Delta\sigma\sqrt{\pi a} + \left[\int_0^a h(x, y, a) \cdot \{E \cdot t \cdot T \cdot d_{31} \cdot \Delta V / A \cdot t_P \cdot (\psi + \alpha)\} \cdot \mathrm{d}x \right] \right\} \cdot F\left(\frac{a}{W}\right).$$

The second term of the above equation provides the change in SIF under the application of voltage which is a negative quantity. The second term vanishes when VR = 1.0 as $\Delta V = 0$. In order to minimize ΔK, ΔV must be maintained at a higher value which results in low FCGR. To maximize the fatigue life, $K_{\max}$ is to be lowered by applying a higher $V_{\max}$. So, for the best repair performance, $V_{\min}$ should be equal to zero i.e., VR = 0 to maintain maximum ΔV for a fixed value of $V_{\max}$. Furthermore, the findings show that even at constant voltage, where there is no change in ΔK, a slight increase in fatigue life is obtained. This is because the application of constant voltage lowers $K_{\max}$, i.e., $(K_{A,\max})_{at500V} < (K_{I,\max})_{withoutrepair}$ and more cycles are required to reach K_{IC}.

6.3.2 Effect of Patch Thickness

The thickness of piezoelectric actuators plays an important role in repair performance. It was reported in previous research [18, 24] that thin actuators with high voltage provide the best result. This happens because the compressive force produced at the crack surface by the piezoelectric patch is inversely proportional to the thickness of the patch. For this reason, a 500 V maximum voltage ($V_{\max}$) is taken to study the effect of piezoelectric patch thickness for t_P = 0.5, 0.75, and 1 mm. The change in final crack length with respect to

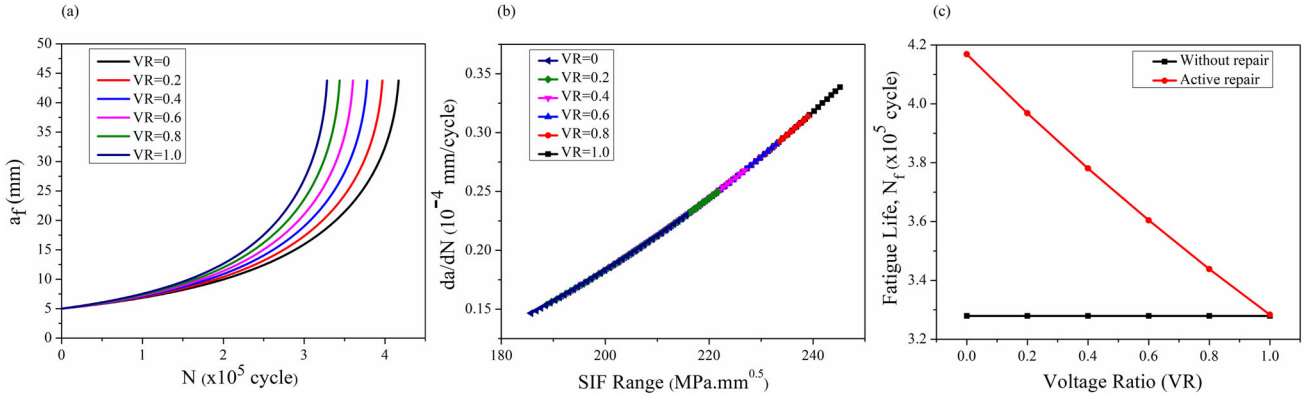

Fig. 14 Results of active repair for various voltage ratios keeping V_{max} = 500V **a** crack length vs loading cycle, **b** fatigue crack growth rate vs SIF range, **c** fatigue life

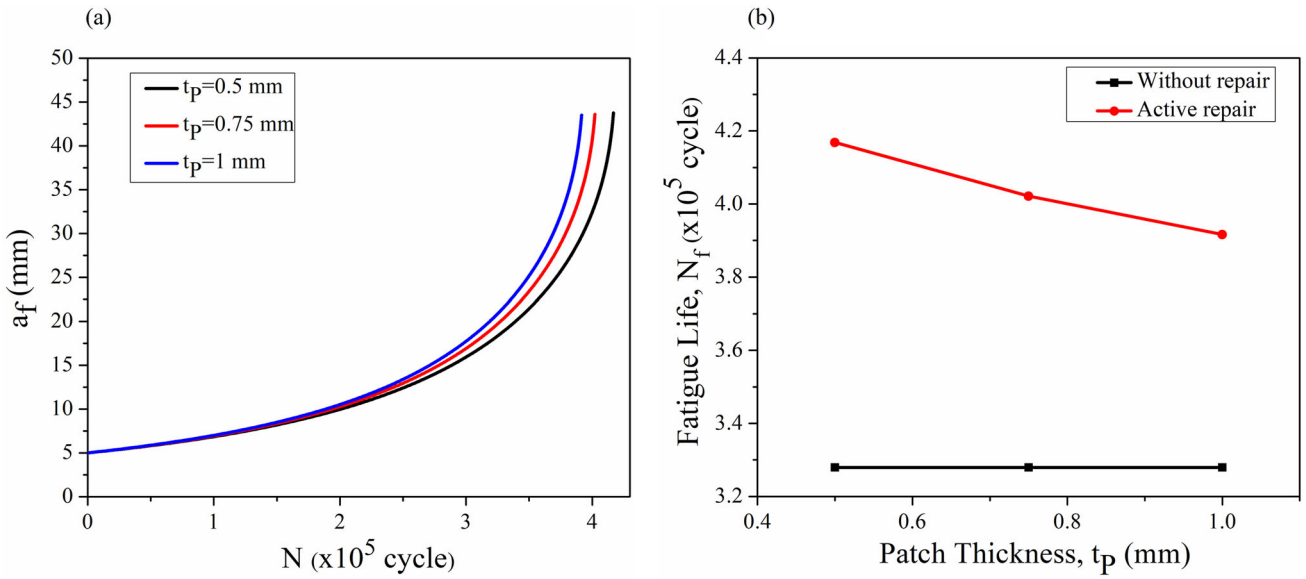

Fig. 15 Results of active repair for different patch thicknesses **a** crack length vs. loading cycle, **b** fatigue life

the number of loading cycles is shown in Fig. 15a. The fatigue life is decreased by 3.53% for the case when the piezoelectric patch is increased from 0.5 to 0.75 mm, 6.05% for the case when the piezoelectric patch is increased from 0.5 to 1 mm, and 2.61% when it is changed from 0.75 to 1 mm as shown in Fig. 15b.

6.3.3 Effect of Maximum Externally Applied Voltage

For the investigation of the effect of the maximum applied voltage applied to the patch on performance, investigation has been carried out by varying the maximum voltage (V_{max}) from 500 to 1000 V. The piezoelectric patch thickness is kept at 0.5 mm. Crack length is calculated against several loading cycles for the plate only under actuation (active repair) as represented in Fig. 16a. The variation in FCGR (da/dN) with respect to SIF range (ΔK) within 10^5 cycles is plotted in Fig. 16b, and lower crack growth is observed for the higher applied voltage. This is found due to the higher reduction in stress at the crack tip hence lowering the SIF.

According to Fig. 17a, the fatigue life extends as the applied external voltage rises. The findings indicate that the fatigue life can be enhanced by 27.12, 33.68, 40.7, 48.22, 56.27, and 64.92% for the voltages 500, 600, 700, 800, 900, and 1000 V, respectively, with respect to without repair condition as shown in Fig. 17b. The percentage increase in fatigue life when applied external voltages are increased from 500 V is summarized in Fig. 17b. It is found that the fatigue life is improved by 5.16, 10.6, 16.5, 22.9, and 29.73% when the applied voltage is increased by an amount of 100, 200, 300, 400, and 500 V, respectively, from the applied voltage of 500 V. It has been observed that for each 100 V rise, fatigue life could have increased by around 5–7% for this repair configuration.

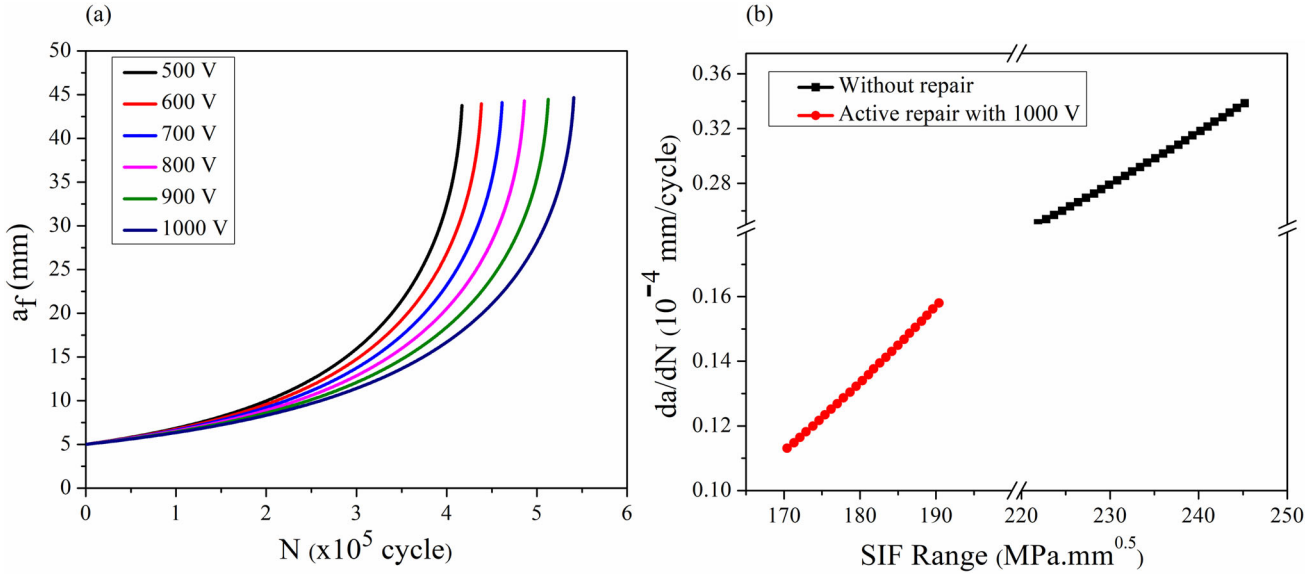

Fig. 16 Results of active repair for various applied external maximum voltages **a** crack length vs loading cycle, **b** fatigue crack growth rate vs SIF range

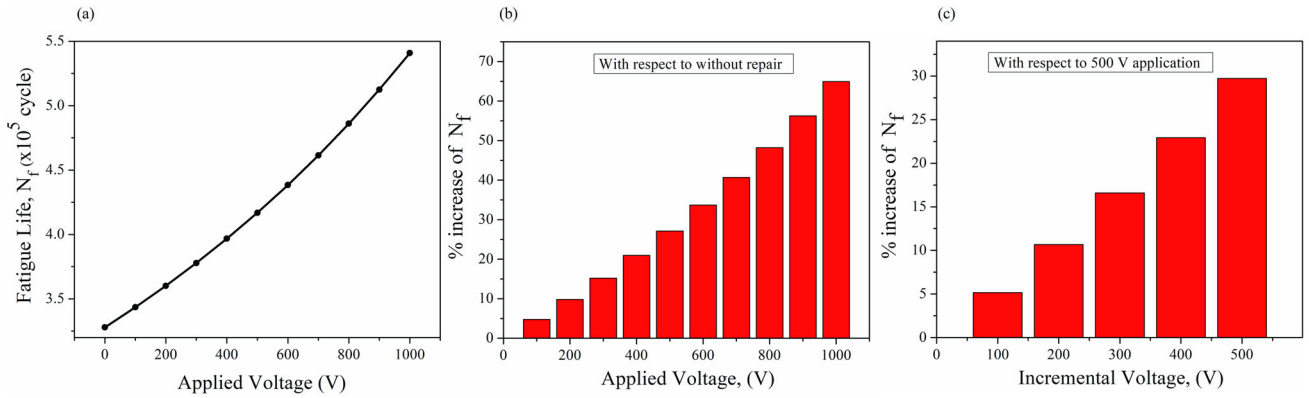

Fig. 17 **a** Fatigue life for different external applied voltage, **b** increase in fatigue life different external applied voltage compared to without repair, **c** increase in fatigue life for incremental applied voltages with respect to 500 V application

The plate structure, crack geometry, and applied mechanical load figure out the voltage requirement, and a suitable range of external voltage is chosen accordingly. As there is no absolute higher limit of applied voltage, this study is limited to the applied maximum voltage of 1000 V.

6.4 Fatigue Life of Hybrid Repair

It is clear from the results of the previous sections that an increase in patch thickness (t_P) results in a longer fatigue life for passive repair. Section 6.3 shows that increasing t_P will reduce the fatigue life in the case of only active repair given that the piezoelectric patch produces less strain at higher t_P. Results from the hybrid repair methodology, which combines passive and active repair, are reported in this section. To achieve the best performance, an optimal value of t_P must be maintained. Additionally, it has been found that zero voltage ratio (VR) offers the best repair and subsequently a longer fatigue life.

The crack length corresponding to the loading cycle is calculated with $t_P = 0.5$ mm and zero voltage ratio as represented in Fig. 18a for various applied voltages in connection with a without repair case. The number of loading cycles required to reach the critical crack length increases as the externally applied voltages increase as well. Under 100, 500, and 1000 V applications, hybrid repair enhances fatigue life by 111.95, 174.88, and 294.92%, respectively, as compared to without repair conditions. The change in crack growth rate against the SIF range within 3×10^5 cycles is also determined and plotted in Fig. 18b for the cases such as without repair and hybrid repair with 500 and 1000 V. It can be highlighted

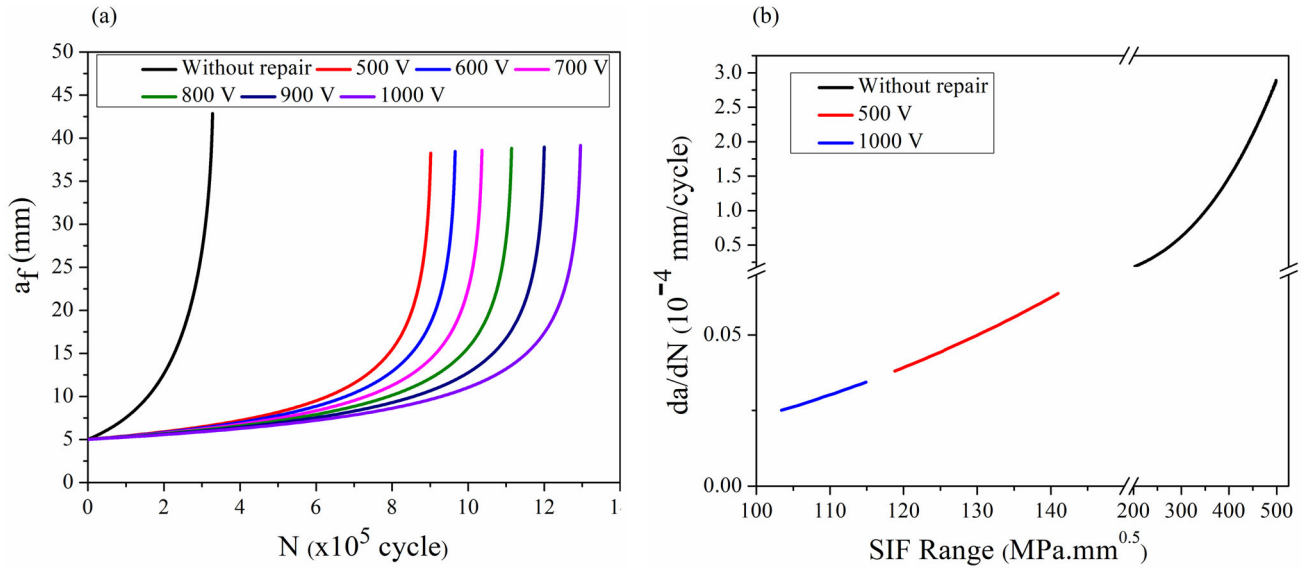

Fig. 18 Results of hybrid repair for various applied voltages **a** Crack length vs. loading cycle, **b** fatigue crack growth rate vs. SIF range

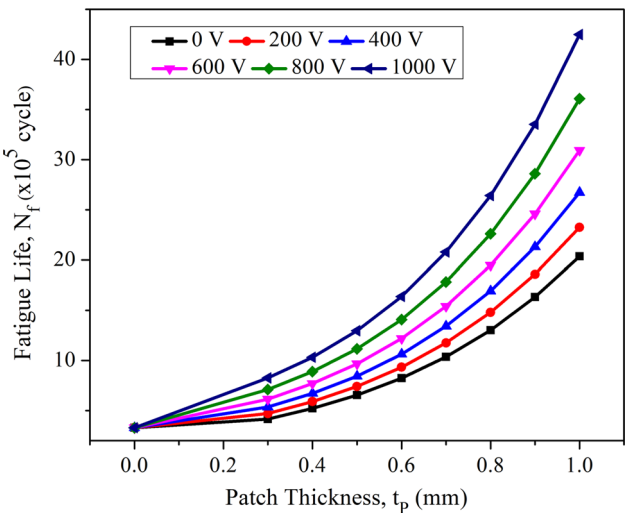

Fig. 19 Fatigue life vs. patch thickness for various applied voltages in a hybrid repair case

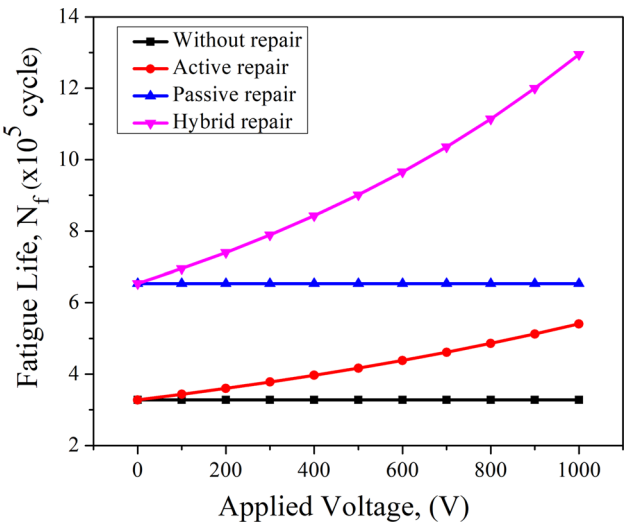

Fig. 20 Variation in fatigue life about the applied external voltage for all repair techniques

that the rise in voltage significantly slows the crack growth rate and thus improves fatigue life.

Figure 19 represents the variation in the fatigue life with respect to the patch thickness for different applied external voltages, and it has been found that better fatigue life is obtained for the higher t_P and external voltage as well. Despite the fact that the results show that higher thickness leads to better fatigue life, it is preferable to choose an optimum lower thickness. This is because if a higher thickness is selected, then the passive effect remains unaffected even if the mechanical load increases while actuation is reduced due to its high thickness. And if a lower thickness is chosen, then the passive effect is slightly reduced, but the actuation effect can be enhanced by raising the external applied voltages as it provides better actuation for thin patches.

In this repair method, the influence of the external voltage is an important consideration. The proper voltage range is chosen following the mechanical loading and desired service life. Figure 20 depicts the fatigue life relative to the different applied external voltage for all repair methods while maintaining $t_P = 0.5$ mm and VR = 0 to show a more detailed illustration. Since the fatigue life of passive repair and without repair conditions is independent of voltage, a constant fatigue life has been found for these cases as shown in Fig. 20. The results of hybrid repair are identical to those of passive repair if no voltage is applied to the patch, simulating the

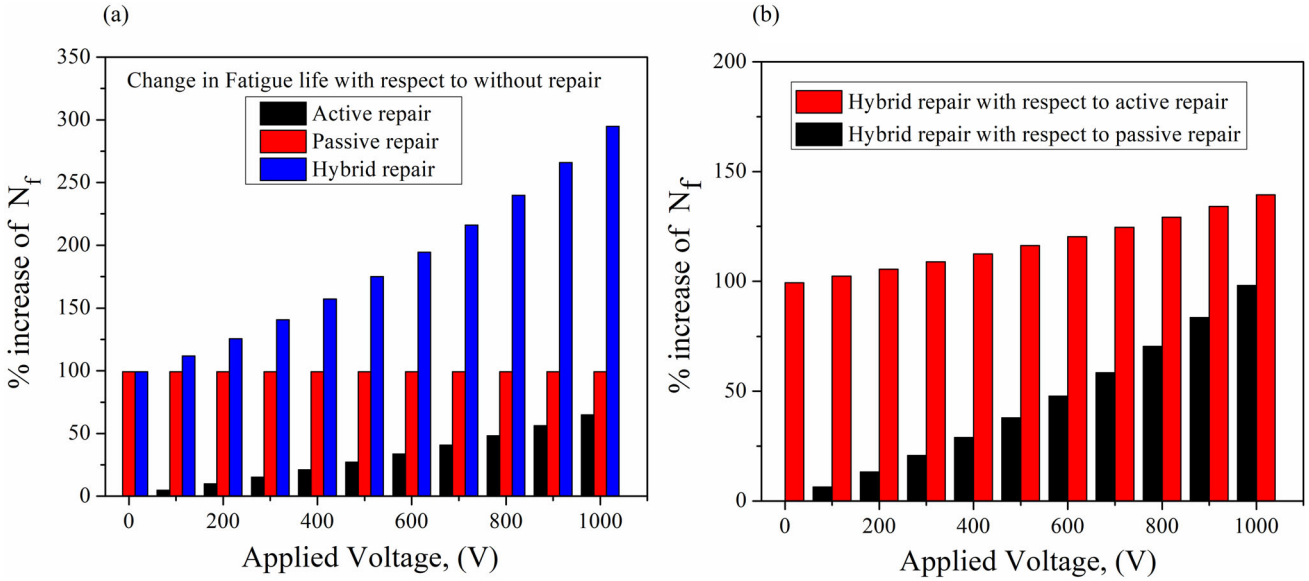

Fig. 21 Percentage increase in fatigue life for different applied external voltages **a** hybrid, active, and passive repair over without repair, **b** hybrid repair over active and passive repair

situation where the plate is not given any actuation. A significant improvement in fatigue life is observed with a rise in voltage as the actuation delivered to the plate encounters the action while the passive effect remains unchanged.

Additionally, an illustration is provided to demonstrate how well active, passive, and hybrid repairs perform in comparison to those without repair. The percentage increase in fatigue life for different repair cases compared to without repair for various external voltages is reported in Fig. 21a. Hybrid repair provides maximum fatigue life enhancement as compared to other repair methods. It is observed that hybrid, passive, and active repairs exhibit 174.88, 99.31, and 27.12% improvement in fatigue life, respectively, as compared to without repair conditions under the application of 500 V. Passive repair is found to have a constant increase in fatigue life than without repair, and this findings hold across all voltages because passive repair has no actuation effect.

Since it is obvious that hybrid repair provides the best performance, another illustration has been made to demonstrate how well a hybrid repair can deliver longer service life when compared to passive and active repair, as depicted in Fig. 21b. In contrast with passive repair, hybrid repair shows 6.34, 37.92, and 98.14% enhanced fatigue life under 100, 500, and 1000 V applications. Furthermore, hybrid repair shows 102.32, 116.23, and 139.46% improved fatigue life in comparison with active repair under 100, 500, and 1000 V applications.

When the applied voltage is increased from 0 to 100, the fatigue life is increased by 6.34%. When 500 and 1000 V are applied, the fatigue life is increased by 29.69 and 86.32%, respectively, with respect to 100 V applications. Fatigue life increases by 43.67% when the voltage is increased from 500 to 1000 V. Every 100 V increase leads to a 6 to 8% rise in fatigue life. This change is found to be slightly higher at higher voltages, which could be due to the dominance of the actuation effect over the passive effect.

7 Conclusions

The reverse piezoelectric effect is used to develop an analytical model for repairing a double-edged cracked infinite plate. The hybrid repair is carried out by taking into account the actuation effect as well as the passive effect of the patch due to its strong bond with the cracked plate. The combined effect of the patch sharing the external load and the compressive stress caused by the actuation of the piezoelectric patch under external voltage results in a significant reduction in stress at the crack tip. This investigation is conducted under cyclic tensile load with $R = 0.1$ and various voltage ratios. Afterward, a validation study is carried out to examine the accuracy of the proposed analytical model using ABAQUS FE solutions and published experimental results. The following conclusions are drawn from the results:

- The investigation demonstrates that different repair techniques, such as active, passive, and hybrid repair, improve the fatigue life of the cracked structure in contrast to without repair. The hybrid repair case exhibits the best performance.
- The passive effect can extend the service life. The thickness of the patch and adhesive also has an impact on the

repair. The best results are obtained by combining a lower thickness with a larger surface area. Adhesive selection has significance as bond strength largely depends on the adhesive's properties.

- Active repair is very suitable because it provides a wide range of repairs by applying different voltages by placing a single patch to the cracked plate. It can be carried out using constant voltage as well as cyclic voltages. The best fatigue life is obtained with a zero-voltage ratio instead of a constant voltage applied throughout the loading cycle. The higher thickness of the patch reduces the fatigue life.
- The piezoelectric patch performs best when its active and passive effects are combined. The passive effect becomes more significant at low applied voltage, but higher voltage results in a higher actuation effect and thus longer fatigue life. The best suitable thickness is reported because very high thickness at high voltage provides less performance.

Funding No funding was received for conducting this study.

Declarations

Conflict of interests The authors have no competing interests to declare that are relevant to the content of this article.

Appendix A

Shear stress distribution will occur in the y-direction as the crack length is covered by the patch. Rice [54] described the upper bond SIF for an infinite cracked plate with a physical parameter 'c,' and the expression is as follows:

$$K_P = \sigma_P \sqrt{\pi c} \tag{29}$$

where

$$c = \frac{1}{\pi k} \tag{30}$$

where k represents the spring constant and is given by Eq. (31)

$$k = \frac{\beta S}{(1+S)\left(1-\upsilon^2\right)} \tag{31}$$

where υ represents the Poisson's ratio of the cracked rectangular plate and β represents the shear stress transfer length in a characteristic adhesively bonded joint and is given by Eq. (32)

$$\beta = \sqrt{\frac{G_A}{t_A}\left(\frac{1}{E_P t_P} + \frac{1}{Et}\right)} \tag{32}$$

where G_A and t_A are the shear modulus and adhesive thickness, respectively. From Eqs. (30) and (31), 'c' can be written as

$$c = \frac{(1+S)}{S} \cdot \frac{\left(1-\upsilon^2\right)}{\pi\beta} \tag{33}$$

Because Eq. (29) is determined for an infinite crack length, the resultant SIF is for the top bond to the infinite cracked Plate. These estimations are restrained due to the patch's reinforcing effect. As a result, the calculated findings are the lowest SIF bound for an infinite cracked plate reinforced by a single-sided patch [49]. For an arbitrary crack length, the following equation has been developed to compute the SIF for an infinite cracked plate using a single-sided patch [48, 49].

$$K_P = \sigma_P \cdot \sqrt{\frac{\pi ac}{a+c}} \tag{34}$$

When the crack becomes extremely short, the results obtained from Eq. (34) are close to the results that were obtained from Eq. (1). When the crack's length is relatively long, the calculated results of Eq. (34) provide the same findings as Eq. (29). This research demonstrates that Eq. (34) falls inside the upper and lower bounds as described by ref. [6].

Appendix B

The bending correction factor (BCF) is given by [1]

$$\mathrm{BCF} = a \cdot y_{\max} \cdot \left(1 - \frac{K_P}{K_I}\right) \cdot \frac{t \cdot (t + t_P)}{I} \tag{35}$$

where y_{max} is the distance of the extreme fibers of the cracked plate from the neutral axis given by Eq. (36)

$$y_{\max} = t + Z \tag{36}$$

where

$$Z = S \cdot \frac{(t + t_P + 2t_A)}{2(1+S)} \tag{37}$$

'I' is the moment of inertia of the repaired plate given by Eq. (38).

$$I = I_{\mathrm{Plate}} + n.I_{\mathrm{Patch}} \tag{38}$$

I_{Plate} and I_{Patch} are the moment of inertia of plate and patch, respectively, and n is ratio of modulus of elasticity.where

$$n = \frac{E_P}{E} \tag{39}$$

$$I_{\text{Plate}} = W \cdot \frac{t^3}{12} + W_P \cdot t \cdot Z^2 \tag{40}$$

$$I_{\text{Patch}} = W_P \cdot \frac{t_P^3}{12} + W_P \cdot t_P \cdot \frac{\left[\frac{t_P}{2} + t_A + \left(\frac{t}{2} - Z\right)\right]^2}{4} \tag{41}$$

Combining Eqs. (35) to (41), the parameter BCF can be found and the modified SIF after passive repair can be expressed as:

$$K_P^* = (1 + \text{BCF}) \cdot \frac{\sigma_0}{1+S} \cdot \sqrt{\frac{\pi ac}{a+c}} \cdot F\left(\frac{a}{W}\right) \tag{42}$$

Appendix C

For any boundary condition, K_{Piezo} can be computed once WFM is known for a particular geometry from Eq. (12). The weight function of a system with a cracked linear elastic body under a symmetrical load needs knowledge of the reference SIF from Eq. (1) as well as the specific geometry's Mode-I stress system. The reference SIF under the action of σ_{Piezo} can be written as

$$K_r = \sigma_{\text{Piezo}} \sqrt{\pi a} \tag{43}$$

The weight function for a 2D cracked structure under Mode-I opening load is as follows:

$$h(x, y, a) = \frac{\acute{E}}{2K_r} \frac{\mathrm{d}u_y}{\mathrm{d}a} \tag{44}$$

where $\acute{E} = E$ for plane stress and $\acute{E} = E/\left(1-\nu^2\right)$ for plane strain conditions. u_y is the plate's displacement in the y direction. The in-plane crack opening displacement for Mode-I opening as per the Westergaard stress function [51] is given as

$$u_y = \pm \frac{2\sigma_{\text{Piezo}}}{\acute{E}} \sqrt{x(a-x)} \tag{45}$$

As the plate is double-edged cracked with crack length a, differentiating u_y with respect to a,

$$\frac{\mathrm{d}u_y}{\mathrm{d}a} = \pm \frac{\sigma_{\text{Piezo}}}{\acute{E}} \sqrt{\frac{x}{a-x}} \tag{46}$$

Now substituting Eqs. (43) and (46) in Eq. (44), the weight function can be found as,

$$h(x, y, a) = \frac{1}{\sqrt{4\pi a}} \sqrt{\frac{x}{a-x}} \tag{47}$$

Piezoelectric actuators are bonded on the cracked plate completely where σ_{Piezo} is the stress produced by the piezoelectric actuators and this stress is having equal perpendicular distribution to the crack surface. d_{31} is the only effective mode which is piezoelectric strain coefficient. Under the application of the external voltage V, the shear force produced by the piezoelectric actuators is given by [10]

$$F_{\text{Piezo}} = \frac{EtT}{\psi + \alpha} \Lambda \tag{48}$$

where T is the distributed electrode width. ψ is a non-dimensional parameter given by Eq. (49). α is a constant that depends on the type of loading and for extensional loading its value is $\alpha = 2$ [10].

$$\psi = \frac{EWt}{E_P W_P t_P} \tag{49}$$

Λ is the piezoelectric strain given by Eq. (50)

$$\Lambda = \frac{d_{31}}{t_P} V \tag{50}$$

σ_{Piezo} can be computed from Eqs. (48)–(50) and is expressed as follows

$$\sigma_{\text{Piezo}} = \frac{EtT}{A(\psi + \alpha)} \frac{d_{31}}{t_P} V \tag{51}$$

where A is the effective cross-sectional area of the plate.

References

1. Ratwani, M.M.: Analysis of cracked, adhesively bonded laminated structures. AIAA J. **17**(9), 988–994 (1979). https://doi.org/10.2514/3.61263
2. Jones, R.; Pitt, S.: Crack patching revisited. Compos. Struct. **76**(3), 218–223 (2006). https://doi.org/10.1016/j.compstruct.2006.06.037
3. Duan, W.H.; Wang, Q.; Quek, S.T.: Applications of piezoelectric materials in structural health monitoring and repair: selected research examples. Materials **3**(12), 5169–5194 (2010). https://doi.org/10.3390/ma3125169
4. Ouinas, D.; Bouiadjra, B.B.; Serier, B.; SaidBekkouche, M.: Comparison of the effectiveness of boron/epoxy and graphite/epoxy patches for repaired cracks emanating from a semicircular notch edge. Compos. Struct. **80**(4), 514–522 (2007). https://doi.org/10.1016/j.compstruct.2006.07.005
5. Errouane, H.; Sereir, Z.; Chateauneuf, A.: Numerical model for optimal design of composite patch repair of cracked aluminum plates under tension. Int. J. Adhes. Adhes. **49**, 64–72 (2014). https://doi.org/10.1016/j.ijadhadh.2013.12.004
6. Wang, H.T.; Wu, G.; Pang, Y.Y.: Theoretical and numerical study on stress intensity factors for FRP-strengthened steel plates with double-edged cracks. Sensors **18**(7), 2356 (2018). https://doi.org/10.3390/s18072356

7. Yala, A.A.; Demouche, N.; Beddek, S.; Hamid, K.: Full analysis of all composite patch repairing design parameters. Iran. J. Mater. Sci. Eng. **15**(4), 70–77 (2018). https://doi.org/10.22068/IJMSE.15.4.7
8. Aabid, A.; Ibrahim, Y.E.; Hrairi, M.; Ali, J.S.M.: Optimization of structural damage repair with single and double-sided composite patches through the finite element analysis and Taguchi method. Materials **16**(4), 1581 (2023). https://doi.org/10.3390/ma16041581
9. Yao, L.; Cui, X.; Zhang, H.; Liu, H.; Wang, C.; He, W.; Xu, J.; Huang, J.: Experimental and numerical investigations of GFRP-repaired short steel tubes with dented damage under axial loading. Mech. Adv. Mater. Struct. **14**, 1–19 (2022). https://doi.org/10.1080/15376494.2022.2158406
10. Crawley, E.F.; De Luis, J.: Use of piezoelectric actuators as elements of intelligent structures. AIAA J. **25**(10), 1373–1385 (1987). https://doi.org/10.2514/3.9792
11. Wang, Q.; Quek, S.T.; Liew, K.M.: On the repair of a cracked beam with a piezoelectric patch. Smart Mater. Struct. **11**(3), 311 (2002). https://doi.org/10.1088/0964-1726/11/3/311
12. Wang, Q.; Chase, J.G.: Buckling analysis of cracked column structures and piezoelectric-based repair and enhancement of axial load capacity. Int. J. Struct. Stability Dyn. **03**(01), 17–33 (2003). https://doi.org/10.1142/s0219455403000793
13. Wang, Q.; Duan, W.H.; Quek, S.T.: Repair of notched beam under dynamic load using piezoelectric patch. Int. J. Mech. Sci. **46**(10), 1517–1533 (2004). https://doi.org/10.1016/j.ijmecsci.2004.09.012
14. Liu, T.J.C.: Crack repair performance of piezoelectric actuator estimated by slope continuity and fracture mechanics. Eng. Fract. Mech. **75**(8), 2566–2574 (2008). https://doi.org/10.1016/j.engfracmech.2007.11.004
15. Wu, N.; Wang, Q.: Repair of a delaminated plate under static loading with piezoelectric patches. Smart Mater. Struct. **19**(10), 105025 (2010). https://doi.org/10.1088/0964-1726/19/10/105025
16. Wu, N.; Wang, Q.: Repair of vibrating delaminated beam structures using piezoelectric patches. Smart Mater. Struct. **19**(3), 035027 (2010). https://doi.org/10.1088/0964-1726/19/3/035027
17. Wu, N.; Wang, Q.: An experimental study on the repair of a notched beam subjected to dynamic loading with piezoelectric patches. Smart Mater. Struct. **20**(11), 115023 (2011). https://doi.org/10.1088/0964-1726/20/11/115023
18. Alaimo, A.; Milazzo, A.; Orlando, C.: On the dynamic behavior of piezoelectric active repair by the boundary element method. J. Intell. Mater. Syst. Struct. **22**(18), 2137–2146 (2011). https://doi.org/10.1177/1045389X11425281
19. Wang, L.; Bai, R.; Chen, H.: Analytical modeling of the interface crack between a piezoelectric actuator and an elastic substrate considering shear effects. Int. J. Mech. Sci. **66**, 141–148 (2013). https://doi.org/10.1016/j.ijmecsci.2012.11.002
20. Fesharaki, J.J.; Golabi, S.: Effect of stiffness ratio of piezoelectric patches and plate on stress concentration reduction in a plate with a hole. Mech. Adv. Mater. Struct. **24**(3), 253–259 (2017). https://doi.org/10.1080/15376494.2016.1139214
21. Fesharaki, J.J.; Madani, S.G.; Golabi, S.: Effect of stiffness and thickness ratio of host plate and piezoelectric patches on reduction of the stress concentration factor. Int. J. Adv. Struct. Eng. **8**(3), 229–242 (2016). https://doi.org/10.1007/s40091-016-0125-x
22. Abuzaid, A.; Hrairi, M.; Dawood, M.S.: Modeling approach to evaluating reduction in stress intensity factor in center-cracked plate with piezoelectric actuator patches. J. Intell. Mater. Syst. Struct. **28**(10), 1334–1345 (2017). https://doi.org/10.1177/1045389X16672562
23. Abuzaid, A.; Hrairi, M.; Dawood, M.S.: Experimental and numerical analysis of piezoelectric active repair of edge-cracked plate. J. Intell. Mater. Syst. Struct. **29**(18), 3656–3666 (2018). https://doi.org/10.1177/1045389X18798949
24. Abuzaid, A.; Hrairi, M.; Dawood, M.: Evaluating the reduction of stress intensity factor in center-cracked plates using piezoelectric actuators. Actuators **7**(2), 25 (2018). https://doi.org/10.3390/act7020025
25. Roy, G.; Panigrahi, B.; Pohit, G.: Crack identification in beam-type structural elements using a piezoelectric sensor. Nondestruct. Testing Eval. **36**(6), 597–615 (2021). https://doi.org/10.1080/10589759.2020.1843652
26. Roy, G.; Panigrahi, B.; Pohit, G.: Identification of crack by vibration analysis and restoration of dynamic response in beams using PZT sensor/actuator. Nondestruct. Testing Eval. **38**(2), 211–232 (2023). https://doi.org/10.1080/10589759.2022.2094378
27. Roy, G.; Panigrahi, B.K.; Pohit, G.: Evaluation and repair of cracks on statically loaded beams using piezoelectric actuation. Int. J. Manufact. Mater. Mech. Eng. **11**(1), 34–49 (2021). https://doi.org/10.4018/IJMMME.2021010103
28. Duong, C.N.; Wang, C.H.: On the characterization of fatigue crack growth in a plate with a single-sided repair. J. Eng. Mater. Technol. **126**(2), 192–198 (2004). https://doi.org/10.1115/1.1647129
29. Duong, C.N.; Verhoeven, S.; Guijt, C.B.: Analytical and experimental study of load attractions and fatigue crack growths in two-sided bonded repairs. Compos. Struct. **73**(4), 394–402 (2006). https://doi.org/10.1016/j.compstruct.2005.02.011
30. Li, Z.; Jiang, X.; Hopman, H.; Zhu, L.; Liu, Z.: External surface cracked offshore steel pipes reinforced with composite repair system subjected to cyclic bending: an experimental investigation. Theoret. Appl. Fract. Mech. **109**, 102703 (2020). https://doi.org/10.1016/j.tafmec.2020.102703
31. Liu, H.; Al-Mahaidi, R.; Zhao, X.L.: Experimental study of fatigue crack growth behaviour in adhesively reinforced steel structures. Compos. Struct. **90**(1), 12–20 (2009). https://doi.org/10.1016/j.compstruct.2009.02.016
32. Bouiadjra, B.B.; Fekirini, H.; Serier, B.; Benguediab, M.: SIF for inclined cracks repaired with double and single composite patch. Mech. Adv. Mater. Struct. **14**(4), 303–308 (2007). https://doi.org/10.1080/15376490600845454
33. Makwana, A.H.; Shaikh, A.A.; Bakare, A.K.; Chitturi, S.: Investigation of patch hybridization effect on the composite patch repair of a cracked aluminum plate: a pragmatic approach. Mech. Adv. Mater. Struct. **26**(17), 1458–1468 (2019). https://doi.org/10.1080/15376494.2018.1432818
34. Ricci, F.; Franco, F.; Montefusco, N.: Bonded Composite Patch Repairs on Cracked Aluminum Plates: Theory, Modeling and Experiments. In: Attaf, B. (Ed.) Advances in Composite Materials - Ecodesign and Analysis, pp. 445–464. InTech, USA (2011). https://doi.org/10.5772/16227
35. Hafiz, T.A.; Abdel Wahab, M.M.: Predicting the fatigue life of adhesively-bonded composite joints under mode I fracture conditions. In: Vassilopoulos, A.P. (Ed.) Fatigue and Fracture of Adhesively-Bonded Composite Joints, pp. 401–417. Elsevier, USA (2015). https://doi.org/10.1016/B978-0-85709-806-1.00014-8
36. Naghipour, P.: Predicting the fatigue life of adhesively-bonded composite joints under mixed-mode fracture conditions. In: Vassilopoulos, A.P. (Ed.) Fatigue and Fracture of Adhesively-Bonded Composite Joints, pp. 419–441. Elsevier, USA (2015). https://doi.org/10.1016/B978-0-85709-806-1.00015-X
37. Li, Z.; Jiang, X.; Hopman, H.; Zhu, L.; Liu, Z.; Tang, W.: Experimental investigation on FRP-reinforced surface cracked steel plates subjected to cyclic tension. Mech. Adv. Mater. Struct. **28**(24), 2551–2565 (2021). https://doi.org/10.1080/15376494.2020.1746448
38. Valadi, Z.; Bayesteh, H.; Mohammadi, S.: XFEM fracture analysis of cracked pipeline with and without FRP composite repairs. Mech. Adv. Mater. Struct. **27**(22), 1888–1899 (2020). https://doi.org/10.1080/15376494.2018.1529844

39. Deng, J.; Fei, Z.; Wu, Z.; Li, J.; Huang, W.: Integrating SMA and CFRP for fatigue strengthening of edge-cracked steel plates. J. Constr. Steel Res. **206**, 107931 (2023). https://doi.org/10.1016/j.jcsr.2023.107931
40. Albedah, A.; Khan, S.M.A.; Benyahia, F.; Bachir Bouiadjra, B.: Effect of load amplitude change on the fatigue life of cracked Al plate repaired with composite patch. Int. J. Fatigue **88**, 1–9 (2016). https://doi.org/10.1016/j.ijfatigue.2016.03.002
41. Ayatollahi, M.R.; Razavi, N.; Chamani, H.R.: A numerical study on the effect of symmetric crack flank holes on fatigue life extension of a SENT specimen. Fatigue Fract. Eng. Mater. Struct. **37**(10), 1153–1164 (2014). https://doi.org/10.1111/ffe.12199
42. Liu, Z.; Li, Z.; Huang, C.; Jiang, X.: An investigation on the fatigue performance of cracked steel plates reinforced with FRP and stop hole. Mech. Adv. Mater. Struct. **29**(25), 3646–3657 (2022). https://doi.org/10.1080/15376494.2021.1907005
43. Ghafoori, E.; Schumacher, A.; Motavalli, M.: Fatigue behavior of notched steel beams reinforced with bonded CFRP plates: determination of prestressing level for crack arrest. Eng. Struct. **45**, 270–283 (2012). https://doi.org/10.1016/j.engstruct.2012.06.047
44. Kong, D.; Zhou, P.; Li, C.; Hong, B.; Xian, G.: Stress intensity factor of through-wall-cracked steel pipe wrapped with prestressed CFRP composites. Eng. Fract. Mech. **283**, 109218 (2023). https://doi.org/10.1016/j.engfracmech.2023.109218
45. Paris, P.; Erdogan, F.: A critical analysis of crack propagation laws. J. Basic Eng. **85**(4), 528–533 (1963). https://doi.org/10.1115/1.3656900
46. Tada, H.; Paris, P.C.; Irwin, G.R.: The Stress Analysis of Cracks Handbook, 3rd edn. ASME Press, USA (2000) https://doi.org/10.1115/1.801535
47. Rose, L.R.F.; Wang, C.H.: Analytical Methods for Designing Composite Repairs. In: Baker, A.A.; Rose, L.R.F.; Jones, R. (Eds.) Advances in the Bonded Composite Repair of Metallic Aircraft Structure, pp. 137–175. Elsevier, USA (2002). https://doi.org/10.1016/B978-008042699-0/50009-7
48. Rose, L.R.F.: Theoretical analysis of crack patching. In: Baker, A.A.; Jones, R. (Eds.) Bonded Repair of Aircraft Structures Engineering Application of Fracture Mechanics, pp. 77–106. Springer, Dordrecht (1988). https://doi.org/10.1007/978-94-009-2752-0_5
49. Zheng, Y.: Experimental and Theoretical Research on Fatigue Behavior of Steel Structures Strengthened with CFRP. Tsinghua University, Beijing, China (2007)
50. Bueckner, H.F.: A novel principle of the computation of stress intensity factors. Zeitschrift Fuer Angewandte Math. Mech. **50**(9), 529–546 (1970)
51. Anderson, T.L.: Fracture mechanics: fundamentals and applications. CRC Press (2017). https://doi.org/10.1201/9781315370293
52. Kumar, D.; Budarapu, P.R.; Pradhan, A.K.: Numerical analysis of lap shear joints made of functionally graded materials. J. Braz. Soc. Mech. Sci. Eng. **45**(2), 94 (2023). https://doi.org/10.1007/s40430-022-03874-4
53. Siruvuri, S.D.V.S.S.V.; Budarapu, P.R.; Paggi, M.: Influence of cracks on fracture strength and electric power losses in Silicon solar cells at high temperatures: deep machine learning and molecular dynamics approach. Appl. Phys. A **129**(6), 408 (2023). https://doi.org/10.1007/s00339-023-06629-7
54. Rice, J.R.: Some remarks on elastic crack-tip stress fields. Int. J. Solids Struct. **8**(6), 751–758 (1972). https://doi.org/10.1016/0020-7683(72)90040-6